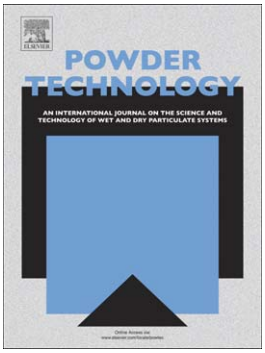

Encapsulation of gases in powder solid matrices and their applications: a review

Thao M. Ho, Tony Howes, Bhesh R. Bhandari

PII: S0032-5910(14)00265-4
DOI: doi: 10.1016/j.powtec.2014.03.054
Reference: PTEC 10142

To appear in: *Powder Technology*

Received date: 4 December 2013
Revised date: 18 March 2014
Accepted date: 21 March 2014

Please cite this article as: Thao M. Ho, Tony Howes, Bhesh R. Bhandari, Encapsulation of gases in powder solid matrices and their applications: a review, *Powder Technology* (2014), doi: 10.1016/j.powtec.2014.03.054

Encapsulation of gases in powder solid matrices and their applications: a review

Thao M. Ho[a], Tony Howes [b], Bhesh R. Bhandari[a *]
[a] School of Agriculture and Food Sciences, The University of Queensland, QLD 4072, Australia
[b] School of Chemical Engineering, The University of Queensland, St. Lucia, QLD 4072, Australia
* Corresponding author. Address: School of Agriculture and Food Sciences, The University of Queensland, Brisbane, QLD 4072, Australia. Tel.: +61 7 33469192; fax: +61 7 33651177. E-mail address: b.bhandari@uq.edu.au (B.R. Bhandari).

Abstract

Gas encapsulation in solid matrices can be an important means to sequester harmful or greenhouse gases and to store useful gases for their subsequent release for a targeted application. In this review, recent developments, the characteristics and gas adsorption capacity of non-organic and organic solid powder matrices (e.g. activated carbons, carbon nanotubes, zeolites, metal-organic frameworks, and cyclodextrins); and potential applications of their complexes in various fields (energy, environment protection, nano-device production, medicine, and food and agriculture productions) are described.

Keywords: gas encapsulation, activated carbons, carbon nanotubes, zeolites, metal-organic frameworks, cyclodextrins.

1. Introduction

Dry atmospheric air consists of approximate volumes of 78.09% nitrogen (N_2), 20.95% oxygen (O_2), 0.93% argon (Ar), 0.03% carbon dioxide (CO_2) and minute traces of neon (Ne), helium (He), methane (CH_4), krypton (Kr), hydrogen (H_2), xenon (Xe) and ozone (O_3) [1]. Some of these gases (such as carbon monoxide (CO), CO_2, CH_4 and nitrous oxide (N_2O)) originate from the incomplete burning of fuels (oil, coal, wood, or natural gases), the widespread use of nitrogenous fertilizers and the industrial manufacturing of nylon. These are the major greenhouse gases which contribute to global warming [1], [2], [3]. Other gases such as sulfur hexafluoride (SF_6) and tetrafluoromethane (CF_4) produced from industrial process are considered as super greenhouse gases having extremely high stability and with the highest potential impact to atmosphere. A gram of SF_6 is climatically equivalent to 24 kg of CO_2 [4], [5]. Other types of gases having high potential hazard as exposure include SO_2, chlorinated volatile organic compounds, and tetrahydrothiophene odorants [6], [7].

Numerous kinds of gases have been used individually, to achieve controlled and selective gaseous atmospheres in a wide range of industries in biology, medicine, science, technology, agricultural and food fields [8]. Methane has been proposed as a possible source of clean energy [9]. Hydrogen is a promising gas in the design of energy-rich fuel-cell devices [10]. Oxygen possesses great importance in diverse areas such as medicine and steel making. Nitrogen is the most commonly used inert gas in biological and food applications, space aircraft and in the ammonia (NH_3) production. Nitrogen, together with Ar and He, is extensively used for running analytical equipment (e.g. gas chromatography) [8], [11]. Nitrogen and CO_2 are also be used to modify the atmosphere in order to control the rate of respiration of agricultural products such as fruits and vegetables to extend their self-life and retard the growth of undesirable organisms during storage [12]. Nitrous oxide (N_2O) is extensively used in anesthesia while nitric oxide (NO) serves as an important messenger in signal

transduction processes in smooth muscle cells and neurons [13], and has antithrombotic effects [14]. Nitrous oxide is also used in canister sprays such as cooking vegetable oil and whipped cream [15], [16]. Carbon dioxide is used as a bubble-creating agent in many kinds of beverage to enhance their organoleptic properties [17], helps to extend the shelf-life and improves the quality of dairy products [18] and orange juice [19], and benefits in blood circulation improvement, blood-vessel dilation and in the activation of gastrointestinal movement [20]. Ethylene (C_2H_4) is also recognized as a useful phytohormone to trigger ripening processes, enhance color development of some types of fruits, de-green citrus fruits and promote germination of many non-dormant seeds (e.g. mung bean sprouts) [21], [22]. By contrast, 1-methylcyclopropene (1-MCP) is an anti-ethylene gas which is used for extending shelf-life and quality of agricultural products [23]. Interestingly, hydrogen sulfide (H_2S) which is the cause of bad smell (especially in rotten eggs) and acid rain [2], is found to be useful for modulating cellular functions [24]. Chlorine dioxide (ClO_2) is used to disinfect objects contaminated by microorganisms (*Bacillus anthracis*) [25]. Ozone (O_3) is used in water treatment and sanitization of raw fruits and vegetable products [26]. The applications of various gases are illustrated in Table 1.

Nevertheless, the use of many of these gases in diverse industries, research and development sectors has many limitations because of their inherent properties. Firstly, the solubility of most of the gases in water and their diffusion in solid materials are usually very low, and are highly dependent on the pressure and temperature. It is therefore very difficult to maintain them with high concentration in solution or solid matrices in desired conditions. Moreover, gases are normally stored and transported in a very high-pressure compressed form in metal cylinders which might be prone to explosion during utilization and transportation. Entrapment of gases in solid matrices would minimize these disadvantages because this can offer safer methods to store for further use and in energy production or emission control. Furthermore, gas encapsulation in powder, granules or pellet form of solid matrices is quite useful in the cases in which a small amount of gas is required.

Entrapment or encapsulation of gases by physical interactions with the host molecules is naturally occurring. It can also be undertaken artificially using man-made solid substrates. In nature, metal-gas interactions, hydrogen bonds and cavity effects exist in many proteins that bind gases [8]. Ability to selectively binding oxygen (O_2) and carbon monoxide (CO) by hemoglobin and myoglobin molecules is a good example of natural physical interactions between gases and the host molecules. Beside iron-gas interactions, the strong hydrogen bonds are also formed between oxygen and the distal histidine of hemoglobin and myoglobin [27]. Entrapment of oxygen in the blood and fixation of nitrogen in leguminous plants are well known examples of gas entrapment in biological systems [27]; [28]. In these systems, the interactions used to form the resultant complexes are noncovalent bonds with weak forces, thus reversible. These forces could be a combination of hydrogen bonding, hydrophobic forces, van der Waals, π-π interactions and electrostatic effects [29].

For the entrapment or encapsulation of gases in artificial solid matrices, numerous attempts are being made to adsorb them artificially in solid matrices for fuel, emission control and ease of use. However, either the concentrations of gas on those matrices are not yet high enough for a commercial interest or the gas does not remain stable in the matrices at the required or desirable conditions. In this review, we present the current status of entrapment or encapsulation of various gases in various artificial solid matrices, and the mechanism of gas adsorption. We will compare the gas storage capacity of various solid matrices. Furthermore, adsorption isotherms, release properties and potential applications of resultant complexes in various fields are discussed. Although there are several solid matrices have been used for gas entrapment, this review focuses mainly on promising solid matrices, namely activated carbons, carbon nanotubes, zeolites, metal-organic frameworks and cyclodextrins.

2. Mechanism of gas adsorption in solid matrices and measurements

2.1. Mechanism of gas adsorption in solid matrices

When gas molecules come in contact to solid matrices, they interact with binding sites on the surface or in cavities of the solid. This process is known as "adsorption" which is completely different with the "absorption" process in which gases directly dissolve into the bulk of the solid. Based on the nature of interactions formed between gases and solid matrices, adsorption is categorized into physical adsorption (physisorption) and chemical adsorption (chemisorption).

In physisorption gas molecules are loosely held by physical forces (dipole-dipole, apolar, electrostatic, hydrophobic associations or Van der Waals). These interactions involve a low sorption energy (8-41 kJ $mole^{-1}$ gas); therefore physisorption is generally reversible and is found in applications in which the useful gases are trapped in solid matrices for their subsequent release for a targeted application. In contrast, in chemisorption the sharing or rearrangement of electron between the adsorbate and the adsorbent can lead to formation of a new substance [30]. The chemical bonds between the gas and the solid surface will have a high sorption energy (62-418 kJ $mole^{-1}$ gas). Thus, an extra energy is required to remove adsorbed gases when they are chemisorbed [24], [31]. The chemisorption is useful in applications where permanently trapping of harmful gases is required. The solid matrices cannot be reused after desorbing gases. For example, lime, limestone or soda limes which produce strong alkali hydroxyls (e.g. $Ca(OH)_2$, KOH, $Mg(OH)_2$ or NaOH) in the presence of moisture can interact chemically with acid gases (CO_2, NO_2 or SO_2) [32], [33]. The differences between physical and chemical adsorption are summarized in Table 2.

Two main factors which govern gas encapsulation in solid matrices are temperature and pressure. In most cases (mainly in physisorption) high pressure is used to push gas molecules to contact at binding sites on the surface or pores of solid matrices. An increase in pressure enhances the adsorption

capacity. The effect of temperature on the adsorption capacity depends greatly on the structure of solid matrices and type of sorption. For instance in hydrogen adsorption on carbon nanotubes, adsorption capacity is higher at lower temperature [36]. In contrast, gas adsorption on zeolite is increased at elevated temperature because the enlargement of pore openings and higher kinetic energy of the gas molecules at high temperature allow gas molecules to diffuse more easily into cavities of solid matrices [37]. Therefore, it is possible to vary the pressure-temperature conditions to optimize the adsorption capacity of solid matrices.

In order to determine the equilibrium absorption capacity for a particular solid matrix, an adsorption isotherm is plotted between the amounts of adsorbed gases as a function of pressure at a constant temperature. The amount of adsorbed gases are expressed in various units, namely weight percentage (wt%); mass, moles or volume per unit mass ([g], [mole] or [cm^3] of gas per [g] of solid matrix respectively); or volume per volume basis (cm^3 of gas per cm^3 of solid matrix) [38]. These adsorption isotherms provide information about adsorption parameters such as surface properties as well as adsorption capacity of a solid matrix [39]. Adsorption behavior of gases on solid matrices is normally described in five general types, as initially proposed by Brunauer et al. (1945) [40], and they can be fitted by many empirical or theoretical models. The most common models are two-parameter models (Langmuir, Freundlich, Dubinin-Raduskevish, Temkin, Flory-Huggins, or Hill), three-parameter models (Sips, Redlich-Peterson, Toth, Khan, Koble-Corrigan, or Radke-Prausnitz), and multilayer physisorption models (Brunauer-Emmett-Teller (BET), Frenkel-Halsey-Hill (FHH), or MacMillan-Teller (MET)) [41]. Depending on the nature or properties of absorbent and adsorbate, one isotherm is better to describe mechanism of adsorption process than others because each of them is constructed based on a different theory or assumption. Table 3 illustrates characteristics of common adsorption isotherms.

2.2. Methods for adsorption/desorption measurements

The amount of gas adsorption/desorption on solid matrices in both single and multicomponent system can be determined by volumetric, gravimetric, oscillometry, thermal desorption or dielectric methods. For studying multicomponent coadsorption, a combination of two or more of these methods is recommended [46], [47], [48], [34]. The theory, experimental setup, examples, advantages and disadvantages of these methods are well described in the books published by Keller and Staudt (2005) [34] and Broom (2011) [49], and are briefly summarized in the proceedings of 2nd Pacific Basin conference on adsorption science and technology (2000) [50]. Therefore, this review only presents the main principles related to these methods.

Volumetric (also known as manometric) and gravimetric techniques are quite similar in operating principle by which both are used to measure the relationship between the amount of gas uptaken by solid matrices and pressure [49]. However, manometric technique is based on the changes in pressure of gas in chamber with known volume containing solid matrices while the gravimetric method is performed by measuring change in the mass of solid matrices kept in a gas chamber with a very sensitive balance [51]. The use of these methods to study gas adsorption equilibrium of various solid matrices has widely been reported [7], [52], [53], [54], [55], [56], [57], [58], [59], [60], [61], [62], [63].

Oscillometry is another technique developed by Keller (1995) for the measurement of gas adsorption on highly porous materials by observing the slow oscillations of a rotational pendulum that attaches the sorbent materials and fixed to a suspension wire. The amount of adsorbed gas is calculated from the frequency and logarithmic reduction of damped oscillations of the pendulum in vacuum and in gas [64], [65]. This technique allows to measure gas uptake at very high temperature and pressure (up to 2,000^{o}C and 100 MPa), even with corrosive gas [50], [34]. The combination of oscillometry with a

volumetric or gravimetric method has also been reported to measure the gas adsorption by swelling polymeric materials [50], [66].

In order to measure the desorption of gas from solid matrices, temperature-programmed desorption (TPD) technique can determine the amount of gas released as a function of temperature by measuring the weight changes of solid matrices under ultra-high vacuum conditions. The gas concentration released from solid materials can be measured by mass spectrometry [64]. This technique includes various analogues such as thermogravimetric analysis (TGA) and thermal desorption spectroscopy, and is well reported for studying the release kinetics of trapped gases (TDS) (TDS) [49] [67], [68], [69], [70], [71], [72], [73].

Another technique for adsorption measurement of gases which have permanent (CO or H_2O) or induced (N_2, Ar or CH_4) dipole moments on porous solids is the dielectric method. The alignment to direction of magnetic field of these gases under an external electric field results in the increase of their dielectric capacity. This technique measures the differences in capacitance of a capacitor filled by solid materials in the chamber with and without gas supply[34]. Many studies on the physisorption equilibria of gases on porous solids using dielectric measurement technique have been reported [74], [75], [76], [77], [78].

Moreover, in order to measure gas adsorption/desorption on water soluble solid matrices such as cyclodextrins, the gas chromatography (GC) measurement is an alternative method. In this method, dissolution of complexes into water in an air-tightly container will release gas into headspace whose composition is subsequently determined by GC. This method was proved to be an effective way to study encapsulation of C_2H_4 into α-cyclodextrin and its release from C_2H_4-α-cyclodextrin complexes [79], [80]. A more practical and cheaper way which can replace for GC to measure gas composition in headspace is the use of gas meters. In present study, we have established a CO_2 measuring system

using CO_2 probe for study adsorption and desorption of CO_2 into cyclodextrins. This system requires fans for air circulation and magnetic stir for agitation. The experimental results show that the CO_2 concentration measured by this system is quite close that determined by GC (data no shown).

3. Solid matrices used for gas encapsulation

3.1. Types of solid matrices

The composition of solid matrices used for gas encapsulation is the major determinant factor of the physical and chemical properties of resultant complexes. Therefore, the ultimate application of complexes is a prerequisite for selecting a solid matrix to adsorb gas. These properties include ability to form interactions with gases, stability of adsorbed gases in the complexes under the operating conditions, gas release characteristics on exposure to a stimulus condition, and cost [81]. A high gas adsorption capacity of solid matrices is required for gas storage while selectivity of a given gas over another is preferred to gas separation. The controlled release of the adsorbed gas molecules is more important in most biomedical, agriculture, horticulture and food applications. An ideal solid matrix should show high storage capacity and it should interact strongly enough with gas to prevent their unintended release due to effects of surrounding environment conditions (especially temperature or humidity) during storage. But the interaction should not be so strong that it is difficult to release the gas in a desired condition for a particular application [13]. In addition, the matrices will be required to be non-toxic, biodegradable, or biocompatible if they are intended to be used in food, pharmaceutical or agriculture systems.

There are numerous types of solid matrices for gas adsorption reported in the literature. These matrices are extremely different in their framework structure composition and properties. Based on their molecular composition, solid matrices can be categorized into non-organic and organic systems [38]; [82]. In addition, they can also be classified depending upon their molecular structure if they are

crystalline or non-crystalline complex matrices. Table 4 provides a classification of the types of matrix material. The non-organic matrices can also have metal ions as binding sites for gas molecules, and are more flexible to tailor gas adsorption capacity than organic systems. There have been a number of attempts made to store various gases by entrapping them in the nanopore or mesopore structures of non-organic or organic systems for fuel and emission control, but encapsulation of gases in biocompatible compounds which is of interest for their unrestricted applications in pharmaceutical, medicine, cosmetics, agriculture and food applications is still in an infant stage in terms of development and application. There are only a few recently published research papers. The reason might be due to the low amount of entrapped gases and instability of inclusion complexes in standard conditions. Furthermore, based on the structure, solid matrices can be classified into an ordered structural group (crystalline) with well-defined pore size (e.g. zeolites and carbon nanotubes), and a disordered structural one (non-crystalline) with a wide range of pore diameters. The structure of materials is well characterized by X-ray diffraction techniques. The level of porosity can be predicted by this X-ray diffraction method and BET adsorption study [83].

3.2. Characteristics of various solid matrices

3.2.1. Activated carbons

3.2.1.1. Molecular structure and mechanism of gas-matrix complexation

Activated carbons (ACs), which are also called activated charcoals or activated coals are prepared from a wide range of high carbon content raw materials such as coal, vegetable, coconut shells, petroleum, wood, polymeric precursors and other agricultural by-products [84]. There are two common ways of producing activated carbons, known as physical and chemical activation. In physical activation two processing steps are involved at high temperature (~973 K), first carbonization of the starting material in an inert atmosphere followed by exposure of this material to an oxidizing atmosphere (steam or

oxygen). In chemical activation, the starting materials are impregnated with a chemical such as H_2SO_4, H_3PO_4, $ZnCl_2$ or alkali metal hydroxides, then carbonized at moderate temperature (673-873 K) [85]. Generally chemical activation is easier and faster to achieve [6].

Activated carbons have an extremely porous structure with a wide range of pore diameters and surface area. The surface area is from 500 to 3000 $m^2 g^{-1}$ depending on the process of activation (physical or chemical activation) [86]. Ranges of porosity are found in the activated carbons, macropores (>500 nm), mesopores (4-500 nm) and micropores (<4 nm) whose proportions can vary significantly according to starting materials (Figure 1). During activated carbon production, macropores are firstly created due to oxidation of weak-interaction groups on the external surface of starting materials, followed by mesopores' formation along the walls of the macropores, and then generation of micropores throughout the structure of the raw material [87]. Under an electron microscope, individual particles of activated carbon not only display various types of porosity, but also show many areas where the graphite-like flat surfaces of particles are intercalated with an interparticulate space of only a few nanometers in which gas molecules can be adsorbed (Figure 2) [88].

3.2.1.2. Gas adsorption property and loading

Activated carbons can exist in various forms including powders, granules, cylindrical extrudates, spherical beads, polymers and fibres. They are the most significant adsorbent materials used to separate and purify gas mixtures, or remove hazardous gases in chemical and petrochemical industries. The findings of these research works summarized in Table 5 indicates that gas adsorption capacity of activated carbons depends essentially on the activation conditions, starting material properties, and concentration of adsorbed gases. At low temperature and pressure (about 0.101 MPa and 273-298 K) activated carbons can adsorb 0.41 g $100g^{-1}$ of SO_2 [82]; 7.00-35.42 g $100g^{-1}$ of CO_2 [55], [90], [91]; 11, 0.18-0.25, and 14.96 g $100g^{-1}$ of ClO_2, chlorpyrifos, and CF_4 respectively [5], [25], [92]. When

increasing in adsorption pressure, some types of activated carbons show quite impressive increase in adsorption capacity such as Maxsorb and coal-based activated carbon which can entrap 143.00 and 80.90 g $100g^{-1}$ of CO_2 at about 3.30 MPa respectively [7], [60]. For gas adsorption, the use of activated carbon has many benefits over other techniques such as wet or dry scrubbing using lime or limestone as absorbents in terms of cost-effectiveness, energy requirement and applicability over a wide range of temperatures and pressures [42], [84]. The mechanism of gas absorption of lime or limestone will be discussed in 3.2.6.

Due to a disordered and energetically heterogeneous internal porous structure, activated carbons' efficiency of gas adsorption in nanospaces can be low [93], especially for large-size gas molecules because they might get stuck at macropore or mesopore channels, making them unable to reach to binding sites in micropores. The heterogeneity of pores can be reduced, and binding sites can be enhanced via modification of activated carbon preparing conditions by a selection of a tailoring method according to the nature of absorbed gases. For example, CO_2 is a Lewis acid therefore removal or neutralization of acidic functionalities of activated carbons by replacing acidic groups with appropriate basic groups (such as basic nitrogen functionalities), can significantly enhance its CO_2 adsorption capacity. The surface modification of activated carbon at various conditions for controlling carbon dioxide adsorption is well reported by many researchers [90], [94], [95], [96], [97] and is reviewed by Shafeeyan et al. (2010) [98].

3.2.1.3. Gas release property of the complex

For releasing gases adsorbed in activated carbons, combination of increase in temperature and/or reduction in pressure is used, which are opposite conditions of adsorption. In the process called "temperature swing adsorption" (TSA) [104] in which gas adsorption is carried out at low temperature, and regeneration of activated carbons is performed by increasing in temperature; however in "pressure

swing adsorption" (PSA) process, regeneration is done by decreasing in pressure [55], [105]. Of these TSA typically requires a longer time to regenerate [106]. Electrothermal swing adsorption which involves direct application of electricity to saturated CO_2 activated carbons, has been found more efficient and easier for desorbing carbon dioxide from activated carbon than by TSA and PSA methods [107]. While the mechanism of gas adsorption on activated carbons are well described by adsorption isotherm models shown in Table 3 [7], [42], [43], [44], [62], just a few of models was proposed to study desorption kinetics. Gay and Do (1989) [108] developed a theoretical model, which is a combination between bimodal (macropore and micropore) diffusion control with a Freundlich isotherm acting at the micropore mouth, to describe gas desorption in a single particle with different geometry and particle size. This model was used to predict SO_2 desorption from activated carbon particles [109].

In thermal reactivation or regeneration of saturated activated carbons the complex is dried firstly at low temperature (about 378 K), followed by pyrolysis at 773-973 K in an inert atmosphere to desorb gas, and then gasification with oxidizing gases (steam or O_2) at a higher temperature (about 1,173 K) to eliminate residual gas completely [110]. The high temperature can burn off about 5-15 (wt%) of the carbon bed for each cycle leading to a loss of adsorption capacity [111]. This process can also transfer the contaminants and change the pore size distribution of activated carbons [112]. In spite of being the most widely described method, thermal reactivation requires a high energy and cost to operate. Alternative approaches, which are believed to lessen the drawbacks of thermal reactivation, are well reported, including wet oxidation [113], electrochemical [112], chemical and solvent [114], ultrasound [115], supercritical [116], and bio-regeneration [117] methods.

3.2.2. Carbon nanotubes

3.2.2.1. Molecular structure and mechanism of gas-matrix complexation

Another solid matrix whose main chemical make-up is similar to that of activated carbons is carbon nanotube. It was discovered in 1991 by Iijima as a tube-like material made of carbon. The tube typically is several micrometers in length and a few nanometers in hollow cavity [118]. A tube can be scrolled by one or several graphene sheets to form the single-walled nanotubes or multi-walled nanotubes respectively (Figure 3) [119]. The both ends of pristine tube are generally locked by fullerene-like half spheres consisting of five- and six-membered carbon rings, limiting the gas molecules' penetration and interaction with binding sites inside of tubes [120]. However, it has been demonstrated that heat treatment in the presence of air leads to open caps at both ends of tubes, improving the gas adsorption capacity significantly [121]. Levesque et al. (2002) compared hydrogen adsorption capacity between a parallel bundle of closed and open carbon nanotubes having the same diameter; and found that for closed carbon nanotubes, adsorption capacity is reduced by a factor of 10 for a nominal diameter (d) of nanotube of 3.4 Å, and by a factor of 2 for d = 6.0 Å [122].

The multi-walled nanotubes with many graphene layers can exist in a wider variety of configuration and shapes with an interlayer spacing of approximately 0.34 nm [123]. Figure 4 illustrates some possible structures of the multi-walled nanotubes. The structure of "Russian doll" (Figure 4a) or "hexahedral prisms" (Figure 4b) include a set of single-walled cylinders or hexahedral prism tubes arranged coaxially one into another respectively, therefore the inner spaces of these structures are out of reach for gas molecule penetration. In contrast, gas molecules can easily access into inner spaces of the multi-walled nanotubes with the structures shown in Figure 4c: papier-mache, which has small graphene fragments assembly, and Figure 4d: scroll, which has a single sheet of graphite rolled in around itself [124]. The gas adsorption of carbon nanotubes has become an integral part for fundamental research, as it has offered a wide range of potential applications including energy storage, emission control, gas separation and nano-electrical devices. The carbon nanotubes have a very high gas storage capacity, because of their compact structure in bundles (Figure 5a) and the existence of

numerous binding sites for interactions with gas molecules (Figure 5b). The binding sites are located inside the nanotubes, on external surfaces of nanotubes, or on spaces among the nanotubes (e.g. interstitial or on the groove that is the space between two or three tubes respectively) [125]. In general, gases adsorbed on the inside and inter-space binding sites are much strongly bound than that on the surface of carbon nanotubes [126]. Shi and Johnson (2003) who studied CH_4, Ar, and Xe adsorption on homogenous (e.g. the same-diameter tubes) and heterogeneous (e.g. a wide range of different-diameter tubes) bundles of carbon nanotubes found that these gases are not adsorbed into the interstitial channels of homogeneous bundles, but do adsorb on interstitial channels of heterogeneous bundles as the latter situation consists of structures with multi-packing defects with relatively large interstitial channels [127].

3.2.2.2. Gas adsorption property and loading

Carbon nanotubes have been found to adsorb a wide variety of gases such as CO_2, Ar, H_2, N_2, tetrafluoromethane (CF_4) and others (Table 6). Interaction between the nanotube surface and gas molecule is based on physical adsorption because of the nonspecific van der Walls interactions [5]. The gases can be highly compressed reaching the density of a solid phase because high pressure results into densification and condensation of the gas inside the pores enhancing the storage capacity significantly. Encapsulation also results in an enhancement of the flexural strength within the nanotube structure due to the presence of a solid or compressed gas inside the tube core. The findings of these research works summarized in Table 6 indicates that in many cases (e.g. CO_2 adsorption) the gas encapsulation capacity of carbon nanotubes is not as high as that of activated carbons, but carbon nanotubes have been demonstrated to be effective solid matrices to entrap many high molecular weight gas molecules. Carbon nanotubes encapsulated 47.68, 55.14, and 34.36 g $100g^{-1}$ of CCl_4, Xe and Kr respectively, at very low pressure and temperature conditions ($(1.1\text{-}2.7)x10^{-4}$ MPa and 77-224

K) [57], [128]. At higher pressures and temperatures, carbon nanotubes were predicted to entrap about 119.77 and 21.12 g $100g^{-1}$ of SF_6 and CF_4 respectively [5], [129]. The adsorption capacity also varies on the treatment of the nanotubes. As a result attempts have been made to modify the nanotubes to increase the high yield of gas storage in nanotubes, such as by creating aligned dense arrays of nanotubes like stack of bamboo structure [130] or by attaching functional amine groups in the side wall of the nanotubes which are able to adsorb carbon dioxide [131]. Dramatic changes in the electronic and transport properties of the carbon nanotubes have been observed after adsorbing charge acceptor gases (O_2 or NO_2), which are essential in manufacturing nano-electronic devices, chemical probes or biosensors [126].

There are some characteristics of the carbon nanotubes that limit their gas adsorption capacity and hinder their further application. Firstly, difficulties in purification during synthesis lead to impurities resulting from the residue of metal catalysts in carbon nanotubes [119]. These impurities, together with water insolubility and non-biodegradable ability has constrained applications of carbon nanotubes in biomedical or food fields to date [132].

3.2.2.3. Gas release property of the complex

Temperature and pressure are two well-known factors for gas desorption from carbon nanotube complexes. Liu et al. (1999) found that at room temperature 73.8% (3.3 g $100g^{-1}$) of the adsorbed hydrogen amount (4.20 g $100g^{-1}$) on single-wall carbon nanotubes was released as the pressure was reduced from 10 MPa to atmospheric pressure, and the remaining adsorbed hydrogen (0.9 g $100g^{-1}$) was only desorbed when the complex was heated up to 473 K [136]. The combination of changes in pressure and temperature to increase the rate of gas release from carbon nanotubes was also reported by Hsu et al. (2010). The time required to release all of the CO_2 adsorbed onto multiwalled carbon nanotubes modified by 3-aminopropyl-triethoxysilane (3.7 g $100g^{-1}$ of CO_2 at 333 K, 0.101 MPa) was

25 minutes by thermal treatment at 393 K, and was 30 minutes by vacuum suction at 0.014 MPa. However, when these two methods were combined, the time for CO_2 release declined significantly to 5 minutes. Interestingly, after 20 cycles of adsorption-regeneration for both treatment ways, the CO_2 adsorption capacity and main properties of multiwalled carbon nanotubes (pore structure and surface functional groups) were almost unchanged [143]. This was also reported for the adsorption capacity of H_2 onto Li- or K-doped carbon nanotubes [141]. One method used to study desorption kinetics of gas from carbon nanotube complexes is thermal desorption spectroscopy (TDS) [144], from which the binding energy and desorption activation energy are determined. For example, by using this method the binding energy of Xe on single-walled carbon nanotube bundles was found about 27 kJ $mole^{-1}$ [144]; the hydrogen desorption activation energy from open- and closed-structure multiwalled carbon nanotubes were -16.5 and -18.5 kJ $mole^{-1}$ respectively [145], from Ni nanoparticle-dispersed multiwalled carbon nanotubes was 31 kJ $mole^{-1}$ [146] and 30.8 kJ $mole^{-1}$ [147]. Unfortunately, no reports on modeling of gas desorption from carbon nanotubes is found. However, gas desorption kinetics from a graphite surface, which is similar to carbon nanotube surface, is well described by zero order models [148], [149].

3.2.3. Zeolites

3.2.3.1. Molecular structure and mechanism of gas-matrix complexation

Zeolites are microporous, 3-D crystalline and hydrated aluminosilicates, in a completely linked framework of tetrahedra. The general empirical formula of zeolites is expressed as $M_{x/n}O*[(AlO_2)_x(SiO_2)_y]*mH_2O$ in which n is the valence of the cation (M), m is the number of water molecules, x and y are the total number of tetrahedra per unit cell (normally x : y = 1-5) [150]. The "tetrahedron" is a basic building unit and includes cations (typically Si^{4+} or Al^{3+}) in the centre and O^{2-} in the corners. They are linked together via highly-flexible apical oxygen interactions to form a more

complex building unit called a "ring". Normally, the number of tetrahedra in a ring determines its name and diameter. A ring built by 10 or 12 tetrahedra is known a 10-ring or 12-ring, and their diameter is 0.56 or 0.73 nm, respectively [151]. The next level of zeolite structure is created via the arrangement of rings in various ways to form a "cage". This cage can be occupied by water molecules and cations (K^+, Na^+, Ca^+ or others). These water molecules and cations have considerable freedom of movement resulting in reversible dehydration and ion exchange respectively [152]. The formation of zeolite structure is illustrated in Figure 6.

There are four common types of cages found in zeolite frameworks namely α-, β-, ε- and super-cage [151]. The β-cage (sodalite cage) and ε-cage (cancrinite cage) are formed by both 4-rings and 6-rings in different arrangements while the α-cage and super-cage are created by connecting 8-rings and 12-rings, respectively. Moreover, the cages can be arranged in cage-to-cage chains to form one-, two- or three-dimensional channels which allows gas molecules to diffuse along their pore [151]. The arrangement of tetrahedra in a large number of ways produces different possible zeolite structures [153]. More than 200 types of zeolites including natural and artificial ones have been identified and their porous networks as well as some properties are clearly described in databases such as "The Database of Zeolite Structures"[154] and "Zeolites and Microporous Structures Characterization" (ZEOMICS) [155].

3.2.3.2. Gas adsorption property and loading

Zeolites known as "molecular sieves" are extensively used in various branches of industry such as the petrochemical and petroleum-refining industries for gas emission control, or gas separation and storage (Table 7) because of their unique properties. The uniformity and wide range of the pore dimensions are determined by the location, size and coordination of the extra-framework cations as well as the arrangement of tetrahedra. They can have a high selective adsorption ability because different forms of

cation can lead to significant differences in the adsorption ability for a particular gas. The pore sizes of zeolite cavities are fixed and are usually small, which reduces their efficiency as adsorbent of large gas molecules such as tetrafluorocarbon. The characteristic sizes of the cage pores and channel apertures have a thermal dependence [150], [151]. At elevated temperatures, the increased thermal vibrations of the atoms in the zeolite framework result in an enlargement of the pore openings. In addition, an increase of kinetic energy of the gas molecules at higher temperature allows gases to diffuse through zeolite apertures [156]. In this case, the encapsulation process includes the forcing of gases into the cavities of zeolite crystals at high temperature and pressure, and consequently gases would be trapped inside when gas-zeolite matrices are cooled to ambient temperature [93]. This might be called as "encapsulation mechanism". However, in the case of encapsulation of gases whose diameter is much smaller than cage aperture size of zeolites, (e.g. Kr in zeolite 5A), another encapsulation mechanism known as "chemifixation mechanism" can be observed. In the latter mechanism, gas molecules are blocked in cavities of zeolites through closure of aperture of the channels under hydrothermal treatment at very high temperature (> 823 K for Kr) which can covert the zeolite structure from a crystal to amorphous state due to thermal reaction of zeolite components [157].

The zeolites can be modified by ion exchange to facilitate the adsorption of some gases. The difference in cation size can affect pore width and consequently the adsorption capacity of zeolites. Weitkamp et al. (1995) investigated the hydrogen adsorption capacity of A-type zeolite as a function of cations. Using Na-A zeolite, they performed ion-exchange with solutions of potassium, rubidium and cesium chloride with degree of 95% for K-A, and 53% for Rb-A and Cs-A respectively, and found that at 573 K and 10 MPa almost no hydrogen was encapsulated in the Cs-A zeolite while the adsorption amount for K-A, Rb-A and Na-A zeolites was 0.051, 0.040 and 0.028 g $100g^{-1}$ respectively [169]. The degree of ion exchange can also lead to a reduction in adsorption capacity; for example hydrogen adsorption capacity in a Na-A zeolite approached zero when the degree of cesium exchange reached 55%; while

adsorption capacity was not affected as degree of cesium exchange was 20% [169]. Similarly, Shang et al. (2010) also found that adsorption capacity for nitrogen and methane by chabazite modified with K^+, Na^+ and Ca^{2+} was significantly affected although there was no remarkable difference in their crystal structure. Ionic K^+ with large size (0.133 nm) causes pore blockage, resulting in preventing gas molecules from diffusing through the window while this phenomenon is not detected with small size Ca^{2+} (0.099 nm) and Na^+ (0.097 nm) ions [63]. Selection of cation type as well as degree for ion exchange process will depend on the nature of encapsulated gases.

The basic frameworks of zeolites are nontoxic materials with high chemical and biological stability, and can form reversible interactions with many molecules including gas molecules [14]. Therefore, zeolites (especially natural zeolite such as clinoptilolite) can be used in medicine for drug delivery [170], for treat stomach ulcers and fasten injury healing process; in agriculture for animal dietary supplement and crop yield enhancement [171]. However, inhalation of zeolite dust can result in respiratory problems [172] and the possible leaching of metal ions present in zeolites into aqueous solution [173] might limit their applications. More extensive studies are needed to ensure that use of zeolites, especially synthesized zeolites for these applications does not cause any problems.

3.2.3.3. Gas release property of the complex

Gas encapsulation process in zeolites is reversible, but it requires either high temperature to open cage apertures again to release gases, or treatment with water or acid [156]. Kalinnikova et al. (1986) proposed two ways to effectively decapsulate N_2 and O_2 from KNaA zeolite by heating the gas-zeolite complexes up to 400-500 K, or by blowing with moist gas at milder temperature (330-350 K) [158]. Release of hydrogen entrapped in NaA, KA and RbA zeolites was almost complete at 480 K, and depends on types of metal ions exchanged into zeolites. At the same temperature (especially at high temperature, >450 K), the H_2 release rate of KA zeolite was significantly higher than that of RbA

zeolite, and was double that of NaA zeolite [169]. Moreover, gas release trigger factors from zeolite complexes are also determined by mechanism of gas-zeolite interactions' formation. Matsuoka et al. (1986) found that when Kr molecules that were fixed into zeolite-types 3A and 5A by "encapsulation mechanism" released remarkably when the Kr-zeolite complexes were immersed in water at room temperature. By moistening the gas-zeolite complexes, the zeolite cations can move easily; resulting in widening cage apertures and subsequent release of the encapsulated gases. However, in cases in which Kr-zeolite complexes were formed by the "chemifixation mechanism", an extremely high temperature (> 1,073 K) was required to recrystallize the amorphous Kr-zeolite matrices, causing release of gases [157]. Furthermore, these authors also concluded that diffusion coefficients of Kr in zeolites which were obtained from Ficks'law can be used for predicting amounts of Kr released from Kr-zeolite complexes in dry air [157]. The activation energy for diffusion of N_2, CO_2, and Ar in 3A zeolite was reported to be 72.38, 54.39 and 66.11 kJ $mole^{-1}$ respectively [67]. In addition, release control for entrapped molecules is also obtained via surface modification by functional groups [174], and altering of zeolite-shell thickness [175].

3.2.4. Metal-organic frameworks

3.2.4.1. Molecular structure and mechanism of gas-matrix complexation

Metal-organic frameworks (MOFs) were discovered by Hoskins and Robson in 1989 [176]. They are crystalline materials composed of metal ions or clusters linked by organic bridging ligands via strongly covalent interactions to form 1-, 2- or 3-dimensional infinite network structures [177]. The structure formation of metal-organic frameworks is shown in Figure 7. The 3-D metal-organic frameworks are of most interest because their voids can accommodate guest molecules for many applications including catalysis, sensor devices, or gas storage and separation [178]. These frameworks are ideal solid matrices for gas separation, storage and purification because of their high uniform pore size typically

ranging from 0.3 up to 4.8 nm and extremely high surface area (6240-10,400 $m^2 g^{-1}$ for MOF-210 for example, significantly higher than maximum surface area of zeolite (904 $m^2 g^{-1}$ for zeolite Y) and activated carbon (2630 $m^2 g^{-1}$)). They also have high porosity (void volumes up to 90%) [179]. They are flexible and easy to modify their structure and properties with respect to the desired application through the changes of the metal centres and/or the organic linkers [180]. There are a wide range of metal ions (Cu^+, Cu^{2+}, Ag^+, Cd^{2+}, Zn^{2+}, Co^{2+}, Li^+, Mg^{2+} or Ni^{2+}) and organic linkers (polycarboxylates, phosphonates, sulfonates, imidazolates, amines, pyridyl or phenolates), which can be selected for designing and synthesizing of metal-organic frameworks [181].

The synthesis of metal-organic frameworks can be accomplished either in liquid phases (water or organic solvent) in a closed vessel at room temperature [183] for heat-labile starting materials, or at high temperature to accelerate the rate of reaction between starting materials, known as hydrothermal [184], solvothermal [185], and microwave-assisted synthesis [186]; or in solid state to control reactivity towards to high yield formation [187]. Moreover, it is also possible to amend their structure for specific purposes after they are synthesized. This can be done by introducing metal ions or desired functional groups into the metal-organic frameworks (in their cavity, organic linker groups or open metal sites). Some examples are replacement of the coordinated molecules by highly polar ligands to enhance adsorption selective capacity for carbon dioxide over nitrogen [188]; coordination of polyethyleneimine into metal-organic frameworks (MIL-101) to accelerate CO_2 adsorption capacity [189]; imprisonment of boron nitride into MIL-53 channels to improve adsorption capacity of H_2 and CO_2 [190]; or changes of N_2, H_2 or CO_2 adsorption capacity of MIL-53 with the introduction of isocyanate and isothiocyanate groups into their structure [191]; or improvement of adsorption selectivity towards to CO_2 over CH_4 of MOF-5 by adding lithium metal (Li) [192]. There are a large number of ways to create numerous types of metal-organic frameworks. This diversity might lead to stability and potential toxicology issues of metal-organic frameworks for biological applications. The

reasons are differences in structure and composition. For example ZIF-8, UiO-66 and MIL-100(Fe) are quite stable in water while MOF-5 degrade in presence of water; and in phosphate buffer (pH = 7.4), Bio-MIL-1,1 and MIL-101(Fe) dissolve quickly while M-CPO-27 remains intact [181]. Therefore, it is very difficult to predict the stability of a particular metal-organic framework based on its structure, which can affect controlled-release property. Moreover, although some preliminary research about toxicology of metal-organic frameworks (Fe-MIL-88 and Fe-MIL-101) on rats did not show any harmful effects; and iron fumarate, with the same chemical composition as metal-organic frameworks Fe-MIL-88A, has been approved as an iron supplement [193]. Similar to zeolites the presence of ion metals in structure may pose potential problems for biological applications because of potential for their leaching.

3.2.4.2. Gas adsorption property and loading

Unlike zeolites in which metal ions are always available to form interactions with gas molecules, the metal ions in metal-organic frameworks are tightly held in pores by covalent interactions with organic bridging ligands, or solvent molecules during their synthesis. Removal of the solvent molecules, termed activation of metal-organic frameworks, can be performed by heat treatment [194] or solvent exchange [195]. This results in a structure of metal-organic frameworks with metal ions which may not be coordinatively saturated, known as open or coordinatively unsaturated metal sites. These sites are important in the enhancement of the gas adsorption capacity [196], [197], [198]. Some selected research publications on the adsorption of various types of gases and vapours in several MOFs solid matrices are summarized in Table 8. Furthermore, a number of published papers have reviewed and compared the adsorption capacity of numerous types of metal-organic frameworks for CO_2 capture, and for CH_4 and H_2 storage [197], [198], [199], [200].

3.2.4.3. Gas release property of the complex

Gas release from metal-organic frameworks can be carried out by decreasing pressure, increasing temperature, or exposing to moisture; and the release rate of guest molecules depends considerably on the size of cavities, rigidity, and solvent solubility of metal-organic frameworks [24]. By using thermal desorption spectroscopy (TDS) method, Panella et al. (2008) found that both metal-organic frameworks Cu-BTC and MOF-5 have two types of size-different cavities (0.5 & 0.9 nm for Cu-BTC, and 0.11 & 0.15 nm for MOF-5) which are binding sites for hydrogen while metal-organic framework MIL-53 possess only one 0.85 nm-size cavity. It was found that hydrogen adsorbed in the larger pore size of metal-organic frameworks required the higher temperature to desorb [73]. Water solubility of metal-organic frameworks also affects the release rate of adsorbed molecules. McKinlay et al. (2008) found that the metal-organic frameworks Co-MOF and Ni-MOF loaded with NO can stable over time at dry atmosphere, but significantly release NO when exposing to moisture, even at only 11 %RH [13]. The replacement of water molecules into the coordinated NO in metal-organic frameworks causes desorption of NO. However, at the similar moisture condition, NO-HKUST-1 complexes release a very small amount of NO [193]. Moreover, the release rate of NO from metal-organic frameworks is also affected by type of metal ions. The NO-Ni-MOF complexes release NO much faster than the NO-Co-MOF complexes [13].

3.2.5. Cyclodextrins

3.2.5.1. Molecular structure and mechanism of gas-matrix complexation

Cyclodextrins are starch derivatives and belong to a group of cyclic oligosaccharides composed of α-(1,4) linked glucopyranose units. These compounds have been recently researched to encapsulate gases although such encapsulation potential was reported in early 1960's [213]. Typical cyclodextrins constitute of 6, 7 and 8 glucopyranose units, known as α-, β-, and γ-cyclodextrins respectively (Figure 8); and their common properties are presented in Table 9. The construction units of cyclodextrins have

a toroidal-like shape with the larger and the smaller openings of the toroid at upper and lower faces exposing to the secondary and primary hydroxyl groups respectively [214].

The interior of the cyclodextrin toroids is considerably less hydrophilic than the aqueous environment, and thus able to host hydrophobic molecules including solids, lipids and gases. In contrast, the exterior is sufficiently hydrophilic to impart cyclodextrins water soluble [217]. The water solubility of γ-cyclodextrins is highest (23.2 g $100mL^{-1}$), being significant higher than that of α- and β-cyclodextrins about 1.5 and 20 times (14.5 and 1.85 g $100mL^{-1}$) respectively [217]. The water solubility of cyclodextrins are significantly dependent on temperature, and models expressing a relationship between water solubility and temperature for each type of cyclodextrin was developed by Astray et al. (2009) [218]. Engulfment of the hydrophobic groups of the guest molecules inside the cavity has been found to improve guest molecules solubility in water [219]. Studies on the toxicity of cyclodextrins have shown that orally administered cyclodextrins are non-toxic due to lack of absorption from the gastrointestinal tract [220]. It is hard for cyclodextrins to permeate biological membranes because of their high molecular weight and the presence of many hydrogen donors and acceptors in their structure [221]. Moreover, cyclodextrins (α-, β-, and γ-types) are categorized as GRAS (Generally Recognized As Safe) in the USA, "natural products" in Japan, and as "novel food" in Australia and New Zealand. Therefore, cyclodextrins are being used in food, pharmaceutical, and chemical industries, as well as agriculture and environmental engineering to encapsulate many hydrophobic compounds aiming to solubilize or stabilize them at expected rate and conditions [221], [222], [223].

Cyclodextrin complexes can be formed either in solution which is used for nearly all guest molecules, or in the crystalline state by forming a paste with water [224]. In solution, cyclodextrin apolar cavities are always occupied by water molecules via energetically unfavourable polar-apolar interactions, and these water molecules are easily displaced by less polar guest molecules [214]. Therefore, the main

driving force for the formation of inclusion complexes is the substitution of the high-enthalpy water molecules in cyclodextrin cavities by hydrophobic guest molecules [218]. There is a difference between cyclodextrin and the previously mentioned solid matrices in that this is an aqueous process, whereas the others were direct gas adsorption.

3.2.5.2. Gas adsorption property and loading

Among three forms of cyclodextrins, α-cyclodextrin has the smallest interior cavity (0.47 - 0.53 nm) and is found to be most suitable for forming complexes with organic guests having less than five carbon atoms in their molecules because the smaller cavity will offer the more interaction and better binding force between the guest molecule and walls of cavity [228]. Most common gases have low molecular weight and small size, which can easily fit to the cavity of α-cyclodextrin [226]. Therefore, a number of researchers have reported encapsulation of gases into α-cyclodextrin (Table 10).

The first report about encapsulation of gases into α-cyclodextrin was published by Cramer & Henglein (1956) [213]. Various gases (CH_4, C_2H_6, C_3H_8, Kr, 1-methylcyclopropene, Xe, CO_2 and C_2H_4) were bubbled into α-cyclodextrin solution at controlled pressure (0.7-12 MPa) and temperature (293.15 K) which resulted in encapsulated gas content ranging from 1.04-10.27 g $100g^{-1}$ in crystallized complexes which were collected after 5-7 days of encapsulation [227]. By studying the dynamics of Xe inside α-cyclodextrin cavities, Dubois et al. (2004) [229] found that binding constant of dipolar interactions between Xe and interior cavity was 23±5 (M^{-1}), which close to the value reported by Bartik et al. (1995) [230] of 22.9±6.1 (M^{-1}). In a study by Neoh et al. (2006) [20] they attempted to complex carbon dioxide, a non-polar gas, into α-cyclodextrin either in solid state with different initial moisture content (2, 10 and 30 wt%) at a pressure of 1 or 3 MPa, or in saturated solution of α-cyclodextrin under 3 MPa. The results showed that increase of encapsulating pressure from 1 to 3 MPa had significantly increase in the inclusion ratio while effects of initial moisture content of α-cyclodextrin on inclusion ratio was

not consistent. At 3 MPa, the highest inclusion ratio was observed at sample with 10% of moisture content (5.92 g of gas $100g^{-1}$), higher than at 2% and 30% of moisture content with 5.06 and 4.88 g of gas $100g^{-1}$ respectively. For saturated α-cyclodextrin solution, besides the lowest inclusion ratio (4.79 g of gas $100g^{-1}$), yield of crystalline complexes was only about 56% after 120 hrs of encapsulation. However, complexes crystallized from saturated α-cyclodextrin solution were more stable in all storage humidity condition than complexes produced from solid state of α-cyclodextrin. An increase of storage humidity promoted diffusion of gases consequently increasing the rate of CO_2 release. Having more than 1 mole of CO_2 per 1 mole of α-cyclodextrin indicated that in some molecules of α-cyclodextrin there were more than one CO_2 molecule complexed. By using a similar technique, Ho et al. (2011) [79], [80] complexed ethylene gas in the α-cyclodextrin forming a crystalline complex. This was performed under moderate pressure range of 0.1-1.5 MPa.

As in other encapsulation system mentioned earlier, the yield (crystallized complex recovery) was dependent on the amount of the pressure and the time, in which yield increased with increasing encapsulation pressure and time and reached to equilibrium at value about 45%. In the complex powder, the gas was stable at normal atmospheric condition of temperature and pressure but was sensitive to the humidity above 45% RH. It was possible to predict the release kinetics based on the temperature and humidity of the environment condition. The amount of encapsulated gas was gas : cyclodextrin of 1 : 1 mole which is equivalent to around 2.9% by weight of ethylene (w/w). Gas molecular encapsulation process in α-cyclodextrin solution is a two-step reaction. This reaction involves dissolution of gas into aqueous phase, and formation of inclusion complex in which gas is encapsulated by crystallized α-cyclodextrin. Activation energy required for dissolution of gas will be more than that of diffusion and complexation reactions [225].

There has been no report of the use of β- and γ-cyclodextrins for gas encapsulation. However, cyclodextrins modified by cross-linking with carbonildiimidazole (known as cyclodextrin nanosponges) were found to encapsulate some types of gases because of the changes in channels between cyclodextrins or formation of porous networks during modification process, which can serve as places to occupy gases [231]. These were proved through the research results of Cavalli et al., (2010) [232], who showed that α-, β-, and γ-cyclodextrin cross-linking with carbonildiimidazole at 353-373 K for 4 hrs can also become an oxygen delivery system due to their high oxygen gas storage ability. Moreover, Trotta et al., (2011) [226] found that β-cyclodextrin nanosponges prepared by the similar method can store high amounts of O_2, CO_2 and 1-methylcyclopropene.

The physical interactions such as dipole-dipole bonds, apolar-polar interactions, hydrophobic associations or Van der Waals are found responsible for complexation between host and guest, with no evidence for forming or breaking covalent bonds [233]. Among these interactions, electrostatic and hydrogen bonding significantly affects the shape and structure of complexes. However, depending on particular inclusion complex, some interactions are more important than others. The importance and contribution of each types of bonding to complex formation can be well interpreted via multivariate quantitative structure-activity relationship (QSAR) analyses [234].

In most cases, the complexes are obtained in crystalline form. Followed by the complexation, cyclodextrin inclusion complexes can crystallize in two basically different patterns, the cage and the channel (tunnel) types [235] (Figure 9). The cage type results in when cyclodextrins are packed crosswise or side-by-side, in layers and adjacent layers are displaced by about one half molecules. In each of this molecular arrangement, the internal cavity of a cyclodextrin is locked on both sides by neighboring cyclodextrins further entrapping the guest molecules. On the contrary, channel complexes are formed when cyclodextrins are stacked like coins in a roll (head-to-head or head-to-tail pattern)

therefore cavities line up to produce long channels (tunnels) holding guest molecules. It has been difficult to identify exactly which type of fashion will be formed under a particular condition [236]. However, for α-cyclodextrin, cage type structures are usually formed with small molecular guests while long molecular and ionic guest molecules induce channel- or tunnel-type structures [237]. The tunnel types are generally found for β- and γ-cyclodextrins. The crystal formation is responsible for further locking up of the guest molecule and release property of the complexed gas. Therefore, crystallized complexes were found to be stable for months at normal condition although the storage capacity of gas complexes and obtained yield might not be high enough for actual applications [20], [226], [79]. The hydrophilic cavities of cyclodextrins are not generally able to entrap polar gases such as ammonia (NH_3), sulfur dioxide (SO_2) or hydrogen sulfide (H_2S).

3.2.5.3. Gas release property of the complex

The interactions of guest molecules within the host cyclodextrin are not permanent but rather a dynamic equilibrium [224]. These are the reasons why gases are easily released from complexes. The important environmental factors which have been proved to be effective ways for controlling the releasing rate of gases are humidity and temperature. Increase in humidity and temperature would accelerate the release rate of gases from cyclodextrin inclusion complexes, and gases are almost immediately released upon dissolution in water [17], [20], [80].

Neoh et al. (2006) [20] found that CO_2 release rate from CO_2-α-cyclodextrin complexes under various relative humidity (5, 33 and 75%) was well described by Avrami's equation although this model was initially developed for describing crystallization of polymer [238], and that CO_2 release mechanism was diffusion controlled whose rate was significantly enhanced by high relative humidity. Similarly, in a study on ethylene release kinetics from ethylene-α-cyclodextrin complexes under various relative humidity (52.9, 75.5 and 93.6%) and temperature (318, 338, 358 and 378 K), Binh et al. (2011) [80]

claimed that both Avrami's and power law models can be used to describe ethylene release rate for all conditions, and the former was better fit to experiment data than the latter. A power law model has been commonly used to describe the release rate of solid or liquid components in pharmaceutical products [239]. Moreover, Binh et al. (2011) also found that the amount of energy required to activate ethylene release in inclusion complexes was 65.9 kJ $mole^{-1}$.

3.2.6. Other solid matrices used for gas encapsulation

Other solid matrices used for gas entrapment are calcium-containing inorganic materials known as lime, limestone, or soda limes. They contain or produce strong alkali hydroxyls (e.g. $Ca(OH)_2$, KOH, $Mg(OH)_2$ or NaOH) in the presence of moisture. These alkali hydroxyls interact chemically with acid gases (CO_2, NO_2 or SO_2) from industrial exhaust streams [32], [33]. Unlike previous mentioned solid matrices with high surface area and possessing regeneration possibility, these materials have low surface area with about 2-22.5 m^2 g^{-1} [240] and are generally not reused because of chemical interactions with gases. Normally, lime compounds are used as adsorbents in wet, dry or semi-dry scrubber systems for removal of undesirable gases. In wet systems gas streams are sprayed together with lime solution or are forced to pass through a bulk of lime solution. In dry systems dry powder sorbents are directly injected into the reactor. For semi-dry one, absorbents are first mixed with water to form a slurry which is then injected into the reaction chamber [33]. For these systems, especially for dry and semi dry ones the relative humidity in reaction chamber is a stimulating factor for reaction. The reaction between lime or limestone with SO_2 increases 10 times as relative humidity increases from 20 to 60% [240]. Due to formation of chemical reaction, these matrices were found to adsorb a high amount of gases at normal conditions. For example, by forcing the gas mixture go through a column packed with soda lime for 20 mins, NO_2 and CO_2 adsorption capacity were found about 3.86

and 24.5 g $100g^{-1}$ respectively [32]. However, these matrices are only used for sequestering harmful gases without recycling, and gas entrapment into these matrices generates waste products (solid salts).

Furthermore, encapsulation of gas molecules in the inner spaces of other cavitands (container shaped molecules), (hemi) carcerands and capsules are also reported. In the cavitand groups of molecules (including cyclodextrins which are discussed in the 3.2.5 section), various cavitand matrices are also being reported to encapsulate a number of gas molecules. One of the examples is the calix[4]arene, which are bowl-shaped molecules with shallow clefts and large lattice voids which can encage many gas molecules such as CH_4, CF_4, C_2F_6, CF_3Br and H_2 [241], [242]. The carcerand and hemi-carcerand (cyclic oligomers) are other nano-container molecules which are hollow inside and able to entrap gases [243]. The gas entrapment in carcerand is almost permanent and happens during carcerand synthesis process. Encapsulated gases could not be released from carcerand complexes (also known as carceplexes), even at very high temperature. In contrast, complexes of hemicarcerands (also known as hemicarceplexes) are quite stable at normal conditions and guest molecules are easily released from hemicarceplexes at high temperature [244]. The hemicarcerands and their cavities form reversible noncovalent interactions with gas molecules. For example, cryptophane-A, a type of hemicarcerand, with cavity volume of 0.095 nm^3 can fit easily CH_4 (0.028 nm^3) and Xe (0.042 nm^3) gases [245].

Leontiev et al. (2007) reported a water-soluble hemicarcerand containing two hemispheres connected by methylene bridges with a molecular cavity of around 0.44 x 0.7 nm between two spheres, which was wider than the kinetic diameter of low molecular chain hydrocarbons (0.38-0.43 nm). This makes it possible for an easy flow of the gas or solvent dissolving the gas in and out. Hemicarcerands are water soluble, easy to incorporate gases and also form strong complexes. For example, a simple bubbling of butane gas in a solution of hemicarcerands in water can form around 40% complex [246]. Gas encapsulation can also occur on capsule matrices made up of self-assembly of dimers (e.g. 4,4'-

bis(dimethylamino) benzils or dihydroxytartaric acid disodium salt) which surrounds gas molecules (CH_4, C_2H_4 and Xe) through hydrogen-bonding [247]. The gas adsorption mechanism of these matrices and other synthetic cavities are well reviewed by Rudkevich and Leontiev (2004) [2], [8], [248].

4. Applications of gas-solid matrices

Surprisingly, there are very few actual applications reported on the stored gas in solid matrices to date although promising research works have been published. The reasons might be low adsorption capacity, inappropriate rate of gas release at desired conditions, and toxicity of solid matrices (especially for food, agriculture and pharmaceutical applications). Published research has shown that the storage of gases in solid matrices has high potential for applications in clean energy production, environment protection (emission control and removal of hazardous gases or vapors), nano-devices production, food and agriculture production and pharmacy (Table 11).

4.1. Clean energy production

After the Kyoto Protocol came into effect on 16 February 2005, the development of alternative clean energy sources, instead of fossil fuel, to reduce the amount of emission gases releasing to the air has become an urgent issue for many countries. Some natural gases, such as methane and hydrogen, can be ideal clean energy sources for vehicles because they are lightweight, abundant and almost environmentally harmless [249]. Burning these gases produces very much less amount of toxic gases. However, storage capacity of these gases in solid matrices at expected conditions is still low, although several types of solid matrices (e.g. activated carbons, zeolites and metal-organic frameworks and carbon nanotubes) under various adsorption conditions have been tested (Tables 5, 6, 7, 8 and 10). According to the Energy Efficiency & Renewable Energy (2013), by 2015 and 2017, a single-use

hydrogen storage system (2.0 wt% H_2) [(1)] for portable power applications and onboard automotive hydrogen storage system (5.5 wt% H_2) [(2)], respectively will be developed [250].

As presented in Tables 5, 6, 7, 8 and 10, hydrogen storage of some potential solid matrices can meet these targets however adsorption conditions (temperature and pressure) are far away from expected situations. In zeolite-gas system, based on theoretical calculation, the highest storage ability of hydrogen at 0 K and zero pressure was found for FAU and RHO zeolite types with about 2.86 wt% loading capacity. However, experimental results at atmospheric pressure (0.10 MPa and 77 K) gave loadings which were lower than those figures, with only 1.3 wt% [168]. Interestingly, metal-organic frameworks MOF-177 can adsorb up to 7.50 wt% of hydrogen at 77 K and 7 MPa, which is much higher than the FCTO target [208]. However, decrease in absorption pressure to normal condition (~0.101 MPa) results in significant reduction in absorption capacity of MOF-177, to only 1.52 wt% [207]. Among all solid matrices described above, carbon nanotubes are likely to be the most effective one to store hydrogen because their hydrogen adsorption capacity is very high, especially at low temperature (77-80 K) and high pressure (>7 MPa) which ranged from 4.50 wt% to 8.00 wt% (as shown in Table 6), and simulation results at 77 K and 7 MPa indicated that triangular array open single walled nanotubes can store up to 33 wt% of hydrogen. Nevertheless, increasing the adsorption temperature would lead to decline markedly in hydrogen storage capacity of carbon nanotubes. For example, at room temperature (~298.15 K), even at high pressure (>10 MPa), hydrogen storage capacity was found only 0.90-4.20 wt%. Carbon nanotubes doped with alkali metals such as lithium (Li) or potassium (K) ion have shown extremely high hydrogen uptake capacities at ambient pressure and 313 K or 673 K which was 14 or 20 wt% respectively [141], which are well above the FCTO target. The explanations for this phenomenon might be catalytic effects of alkali metals (Li or K) as

(1) & (2) : These values are on a solid matrix weight basis

well as open-ends and layer-structure of carbon nanotubes. However, releasing hydrogen from these samples required much higher temperatures [141].

For methane, in order to be used as a clean energy source its storage capacity should be as high as compressed natural gas capacity (35 wt%) [38], and therefore almost no present solid matrices can meet that requirement (Tables 5, 6, 7, 8 and 10). Among activated carbon types, the highest methane absorption capacity was found only 21.65 wt% and 23 wt% for Maxsorb (3.3 MPa & 273 K) and coal-based activated carbon (8.5 MPa & 284.3 K), respectively [7], [60]. At similar adsorption conditions (3.65 MPa & 298 K), metal-organic frameworks IRMOF-6 can adsorb about 17.1 wt% [204], which is the maximum value among all types of metal-organic frameworks. The methane storage ability of zeolite and carbon nanotubes is much less than that of activated carbon and metal-organic frameworks. Carbon nanotube adsorbed only 7.62 wt% at 1.72×10^{-3} MPa and 78.7 K [128] while zeolite 3A was predicted to store about 6.90 wt% methane at extremely high temperature and pressure (410 MPa & 623 K) [156]. As shown in Table 7, methane adsorption capacity of the other types of zeolite is quite well below this value.

In summary, in order to be practically used for clean energy, further improvement in storage capacity is required. It is known that gas adsorption capacity of solid matrices depends primarily on number of factors such as surface area, free volume, framework density and heats of adsorption [38]. These will be the basis for further improvements.

4.2. Environmental protection

Application of gas storage in solid matrices for environmental protection implies removal of gases which can be either greenhouse gases (CO_2, CF_4 or SF_6) or hazardous gases and vapors (SO_2, chlorinated volatile organic compounds, and tertbutyl mercaptan or tetrahydrothiophene odorants) from flue gases or exhaust to prevent their detrimental effects to the environment. For this application,

high adsorption capacity, high adsorption selectivity and high interaction energy are expected [38]. Among reported solid matrices, activated carbon seems to be the most effective matrix for this application. The first reason is its high carbon dioxide adsorption capacity. Activated carbon Maxsorb (surface area of 3250 m^2 g^{-1}) could adsorb 143 g $100g^{-1}$ at 3.3 MPa and 273 K [60], closely followed by a coal-based activated carbon (surface area of 1342 m^2 g^{-1}) with an adsorption capacity of 80.9 g $100g^{-1}$ [7]. The adsorption energy for these types of activated carbons is 16-26 kJ mol^{-1} which indicates that interaction between carbon dioxide and activated carbons is strong enough to give reasonable stability at room temperature. Moreover, activated carbon can absorb other toxic gases such as SO_2, ClO_2, tertbutyl mercaptan (TBM) or tetrahydrothiophene (THT) odorants, chlorinated volatile organic compounds and chlorpyrifos to some extent (Table 5). Therefore, activated carbon can be used to eliminate effectively these compounds out of environment. Although carbon nanotubes shows significantly lower carbon dioxide adsorption capacity than activated carbons, they have high potential ability for entrapping other greenhouse gases such as CF_4 and SF_6, with 21 and 119 g $100g^{-1}$ respectively; and toxic gasses such as carbon tetrachloride - (CCl_4) with 47.68 g $100g^{-1}$. Cyclodextrins can adsorb up to 5.87 g $100g^{-1}$ carbon dioxide [227], but they are unable to be used for this application as CO_2-cyclodextrin complexes are not stable at normal operating conditions [225]. They also release carbon dioxide easily under high relative humidity (RH > 75%).

Metal-organic frameworks have the highest surface area among solid matrices, but their carbon dioxide adsorption capacity falls behind activated carbons. At 0.10 MPa the CPO-27-Ni metal-organic framework adsorbs between 12.40 and 29.90 g $100g^{-1}$ CO_2 depending on temperature (303-353 K), which is the highest amount among various types of metal-organic frameworks. Other metal-organic frameworks shown to have ability to interact with carbon dioxide are MIL-53, BNH@MIL-53, Mg-MOF-74, $Zn_2Atz_2(ox)$, MIL-101, PEI-MIL-101, CD-MOF-2 or Zn-MOF at various degree. This proves that diversity and flexibility in modification of metal-organic frameworks structure, which

means that changes in metal ions or incorporation with other component, can result in change in the adsorption capacity. Unlike metal-organic frameworks, carbon dioxide adsorption by most zeolites occurs at a higher pressure. Zeolites 4A and 13X adsorb about 21.10 and 22.90 g $100g^{-1}$ CO_2 at 2.07 MPa and 300 K respectively [55]. For zeolites 13X, when pressure was increased to 5 MPa, its adsorption capacity increased to 32.44 g $100g^{-1}$ [165].

4.3. Nano-device production

Unlike other solid matrices, carbon nanotubes are an amphoteric system which means that they can be doped as an electron donor or electron acceptor once exposed to some types of gases. This charge transfer results in significant changes in the density of free charge carriers, leading to variations of electrical and/or thermal conductivity of carbon nanotubes [251]. This is the basis for production of nanotube molecular devices to detect small concentrations of various types of gases. Gases, which are known to induce charge transfer in contact to carbon nanotubes are O_2, NO_2, NH_3, H_2, N_2, He and Br_2 [251], [252], [253], [254], [255], [256]. The nano-devices detect the presence of gases through measuring electrical resistance, thermoelectric power, or local density of states as a function of exposure time and gas concentration. In order to be used for this application, carbon nanotubes should be metallic, semimetallic or semiconducting. These properties are mainly determined by their chirality, and are only observed in several groups of carbon nanotubes [257], [258].

According to the research findings of Barberio et al. (2009) there is no indication of oxygen adsorption on either clean and pristine or low energy Ne^+ ion bombarded single-walled carbon nanotubes at 298.15 K and 1.3×10^{-10} MPa while the one irradiated with 300 eV O^+ ions showed oxygen chemisorption [134]. In addition, Collins et al. (2000) proved that electrical properties of single-walled carbon nanotubes changed dramatically on exposure to oxygen, which indicated adsorption of oxygen on carbon tubes [259]. Kong (2000) demonstrated the advantages of chemical sensors produced from

semiconducting single-walled carbon nanotubes to detect NO_2 and NH_3 over existing solid-state sensors such as a high-performance metal oxide sensor and poly-pyrole-conducting polymer sensor at room temperature [253] in terms of sensitivity and response time. However, the use of these devices for this purpose still has room for improvement. Slow recovery is one of the limitations as the nano-devices which still require high temperature treatment to desorb gases for the next measurement [253].

4.4. Medical applications

Together with oxygen, four other gases which are proved to have beneficial medical effects are CO_2, H_2S, CO and NO. Carbon dioxide contributes to blood-vessel dilation, blood circulation improvement, activation of gastrointestinal movement, and controlling of blood pressure [20], [260]. H_2S, CO and NO are well-known neurotransmitters, and play an essential role in the regulation of vascular operation [261]. There is no research on storage of CO_2 in solid matrices for medical applications to date. There are only a few studies on H_2S, CO and NO but these still require further extensive studies in terms of storage ability, toxicology and release rate. For medical applications, solid matrices should be free of toxic compounds, capable of storing an appropriate amount of gas, deliver it to specific sites in the body, and release it at a desirable rate through a simple triggering mechanism [173]. Uncontrolled release such as an initial quick release or a very slow release of gases can waste valuable products and do potential harm to the patient [24]. Metal-organic frameworks with high porosity, high biodegradable ability and extremely flexibility in the modification of their structure for intended purposes can be of interest for therapeutic purposes. Moreover, zeolites and cyclodextrins have also being researched to entrap gas for this purpose.

According to Xiao et al. (2007) [173], the metal-organic frameworks HKUST-1 absorbed 3 mmol g^{-1} NO at normal condition (0.101 MPa and 298 K), and in contact with water vapor total amount of NO released from NO-HKUST-1 was only 2 μmol g^{-1}. This amount is found to be very effective in

inhibiting thrombosis formation (1 pmol min^{-1} mm^{-2} of NO) [262]. In an *in vitro* experiment this complex showed significant effectiveness in thwarting thrombosis formation, even after storing this complex in inert environment for up to several weeks [173]. At similar conditions, other metal-organic frameworks Ni-MOF and Co-MOF showed much higher amount of adsorbed NO, which is about 7 mmol g^{-1} NO at 298.15 K and 0.101 MPa [13]. Total amount of NO adsorbed in Ni-MOF or Co-MOF (7 mmol g^{-1} NO) was released after 2 weeks, in which only 1% of its release was in the first hour with trigger factor of humidity of gas (11% RH). This release property is useful in biological application in desiccated environment such as delivery of NO to wound healing on the skin. In phosphate-buffered saline (similar to blood or other physiological solutions), the NO releasing rate from these complexes was much faster, and it took only several hours to release about 50% of total amount of NO absorbed. An *in vitro* study in pig coronary arteries showed NO released from NO-MOFs caused relaxation of arterial tissue [13].

In zeolites, the amount of NO adsorbed is much lower than that of metal-organic frameworks, with only 1.2-1.3 mmol g^{-1} for Co-exchanged zeolite-A at room temperature and 0.101 MPa pressure [14]. The total amount of NO released from zeolite-A can reach 1 mmol g^{-1} NO. NO-releasing-zeolites have been demonstrated to potentially prevent blood clots [14].

There are some concerns for using these zeolites and metal-organic frameworks in medical applications. The first problem is non-dispensability of these systems in the aqueous phase, which may result in difficulties in controlling the release rate as well as in delivering these matrices to target sites. Another concern is the toxicology of metals in frameworks [173]. In order to overcome the first issue, polymers such as poly-tetrafluoroethylene (PTFE) or poly-dimethylsiloxane (PDMS), have been incorporated to these frameworks as binders. This incorporation has only slightly retarded the release rate of gases [14]. Ion exchange of these solid matrices with less- or non-toxic metals could be a means

to reduce concerns about toxicology of solid matrices, especially for metal-organic frameworks. For example Zn ion in Zn-MOFs has been exchanged with other less toxic metals [263].

Allan et al. (2012) studied the applicability of the Ni-CPO-27 and Zn-CPO-27 metal-organic frameworks to entrap H_2S for medical purposes. They found that at 0.101 MPa and 303.15 K, Ni-CPO-27 showed the highest storage capacity of 12 mmol g^{-1} of gas. Following exposure to a moist atmosphere, only 1.8 mmol g^{-1} of H_2S was released from Ni-CPO-27 and 0.5 mmol g^{-1} from the Zn-CPO after 30 minutes; and H_2S release from both CPO-27 stopped after 1 hour with a total release of only a third amount of the adsorbed H_2S. These complexes were stable for more than 9 months with small loss and were still able to release H_2S after this storage period. In an *in vitro* study, foetal calf serum, Zn-CPO-27 incorporated with 10% PTFE polymer, only released H_2S after several minutes of induction. For pig coronary arteries *in vitro* study, the use of a H_2S-Zn-CPO-27 complex stored for 9 months caused vascular relaxation after 5 minutes of induction [211].

In the case of CO gas, although there are some reports on adsorption of CO on zeolites and metal-organic frameworks, they are not likely to be applied in biology. This is due to the very low adsorption capacity of this gas on zeolites and metal-organic frameworks at desired conditions. Britt el al. (2008) claimed that there is no adsorption capacity of CO on several types of metal-organic frameworks (MOF-5, IRMOF-3, MOF-74, MOF-177, MOF-199, IRMOF-62 and BPL carbon) [177]. Zeolite X in forms of ion exchange with Na and Ba absorbed only 2.41 and 2.67 mmol g^{-1} of CO, respectively at 303.45 K and 0.76 MPa, and less than 1 mmol g^{-1} at normal conditions (303.45 K and 0.101 MPa) [161]. Although cyclodextrins are extensively being used for encapsulation of solid and liquid drugs [221], only β-cyclodextrins cross-linked with carbonildiimidazole show the ability to store oxygen for potential *in vivo* application. In this case the complex is coated with silicon membrane to control release rate as well as avoid an initial burst release [226].

4.5. Food and agriculture production applications

Although there are a number of research on encapsulation of solid or liquid compounds in solid matrices for food and agriculture applications [264], gas encapsulation for this purpose is still in an early stage of development. The first application of gas entrapment on solid matrices in food fields is the use of activated carbon and/or other adsorbents such as baking soda (sodium bicarbonate powder), clays or zeolites for deodorization in food storage spaces (e.g. refrigerators, freezers, or other cold storage units) [265], [266]. In these cases, adsorbents are normally packaged into porous and nonwoven pouches, and then placed in posts on back or front panels, or suspended freely of cold storage units. They adsorb unpleasant odors produced by strong smells or spoiled foods via the circulation of air inside freezers.

In cases when adsorbents contact directly to a food ingredient and become a food component, the nature of solid matrices, toxicology, biodegradability, encapsulation capacity, stability of complexes and releasing rate of gas are important criteria which need to be considered [267]. Therefore, only cyclodextrins among all of the solid matrices described earlier are qualified for entrapping gases for direct food applications. In this field, some research has been reported. Ho et al. (2011) complexed ethylene gas (C_2H_4) in α-cyclodextrin at a pressure range of 0.1-1.5 MPa. The amount of encapsulated gas was gas : cyclodextrin of 1 : 1 mole which is equivalent to about 2.9% ethylene by weight (w/w). The complex powder was stable at normal atmospheric condition of temperature and pressure but was sensitive to the humidity above 45% RH. The gas was almost immediately released upon dissolution in water. This inclusion complex has successfully been tested for its applicability in horticulture to promote the ripening process of mangos and germination of mung bean sprouts. Only 100 g of this powder was able to trigger the ripening of 20 tons of mangoes in a container in-transit from a farm to a market located at a long distance [79], [80]. For germination of mung bean sprouts, soaking mung

beans with this powder at a level 0.525-52.5 mg 100 mL^{-1} water significantly improved the rate of seed germination, hypocotyl thickness and uniformity in length of mung bean sprouts [22].

Unlike ethylene, carbon dioxide gas is used in food field to retard the rate of respiration of the agricultural products. Besides, it is a bubble-creating agent in various types of beverage or a leavening agent in some food confections. Although its encapsulation in α-cyclodextrin was earlier patented in Japan in 1987 [226], this work did not lead to a commercial application probably due to the limited storage capacity achieved in applied processes. Neoh et al. (2006) showed that the level of CO_2 encapsulated was 1.25 moles per one mole α-cyclodextrin within a pressure range of 1.0-3.0 MPa, which is much lower than a theoretical value [20]. Based on the theory, the longitudinal molecular size of CO_2 is about 0.232 nm while the internal cavity size of α-cyclodextrin is roughly 0.52 nm diameter and 0.79 nm height; which means more than 2 moles of CO_2 might be entrapped by only a mole of α-cyclodextrin. A low storage capacity of CO_2-α-cyclodextrin complexes is still useful in some cases. In a recent patent, Zeller and Kim (2013) investigated use of CO_2-α-cyclodextrin complexes in cappuccino frothing. They mixed 1.5-3.0 g of complex powder (prepared at 3.4 MPa at 298.15 K for 7 days) to 11.5 g of instant cappuccino mix, and then reconstituted with 150 mL hot water (361.15 K). The froth formation ability of this sample was increased by 2-3 times compared to a sample without adding complexes. A similar result in enhancement of height of froth was observed by adding of N_2O-α-cyclodextrin complexes (encapsulated at 3.4 MPa, 298.15 K for 3 days) in hot instant cappuccino, cocoa, espresso and coffee mixes. Flavor of products with N_2O-α-cyclodextrin complexes was much better than that with CO_2-α-cyclodextrin complexes which induced carbonation and sensation flavor. The stability of froth was mainly determined by foam stabilizers present in milk protein. In another study, mixing of about 3% of N_2O-α-cyclodextrin complex into dough resulted in increasing of oven-baked pizza volume ingredient by 22% with an uniform internal foam structure [17].

Encapsulated gas has also been successfully used in the preparation of powdered soluble foamer by using a mixture of milk, caseinate, maltodextrin, lactose and sucrose [268]. This mixture was moistened to between 15% and 55%, and subjected to extrusion and spray-drying, respectively to create a porous structure which can entrap nitrogen gas at 2 MPa, 343.15 K for 20 minutes. This powder (20% by weight) was mixed with soluble coffee powder and was observed to enhance foam height by about 10 times [268].

Conclusion

This review updated the mechanism and methods of encapsulation of gases in solid matrices and highlighted the opportunity and importance of research in gas encapsulation. Gas encapsulation or adsorption in powder solid matrices can be an important means to sequester harmful or greenhouse gases (SO_2, CO_2, SF_6 or CF_4) and to store useful gases for their subsequent release in a targeted application (H_2, CH_4 or C_2H_4). Numerous types of solid matrices for gas adsorption have been reported in the literature, typically as activated carbons, carbon nanotubes, zeolites, metal-organic frameworks and cyclodextrins. These matrices are extremely different in their framework, structure, composition and properties, and have physical or chemical mechanism of gases on the adsorbent molecules, particle surface or molecular cavity. The gas-adsorbent interaction can be physical or chemical, thus reversible or irreversible respectively. The composition and properties of solid matrices are the major determinant factor of the physical and chemical properties of the resultant complexes. Therefore, the ultimate application of complexes is a prerequisite for selecting a solid matrix to adsorb a gas. Numerous attempts are made to store various gases by entrapping them in inorganic matrices (activated carbons, carbon nanotubes, zeolites and metal-organic frameworks) for environmental protection (harmful or greenhouse gases) and clean energy production (natural gases especially hydrogen and methane). Similarly, examples of gas encapsulation in biocompatible, biodegradable or edible powder matrices

(zeolites, metal-organic frameworks and cyclodextrins) that are significant in medicine, food and agricultural fields have also been reported.

The further application of gas encapsulated in these solid matrices is still limited by their low encapsulation capacity and stability in standard conditions. The high energy requirement for high loading of gas during complexation is another limitation. However, in some cases where a small amount of gases is required for an application, gas encapsulation can be effective due to the availability of gas in a powder format. In the powder form the use of the gas is often more safe and easy to handle, as compared to usual compressed counterpart and offers a wide range of potential applications.

Acknowledgements

The authors are grateful for the financial support of Australia Awards Scholarships.

References

[1]. Subramani, T., Study of air pollution due to vehicle emission in tourism centre. *International Journal of Engineering Research and Applications*, 2012. **3**(2).

[2]. Rudkevich, D.M. and A.V. Leontiev, Molecular encapsulation of gases - a review. *Australian Journal of Chemistry*, 2004. **57**: p. 713–722.

[3]. Miura, Y. and T. Kanno, Emissions of trace gases (CO_2, CO, CH_4, and N_2O) resulting from rice straw burning. *Soil Science and Plant Nutrition*, 1997. **43**(4): p. 849-854.

[4]. Riddell, I.A., et al., Encapsulation, storage and controlled release of sulfur hexafluoride from a metal-organic capsule. *Chemical communications (Cambridge, England)*, 2011. **47**(1): p. 457-9.

[5]. Kowalczyk, P. and R. Holyst, Efficient adsorption of super greenhouse gas (tetrafluoromethane) in carbon nanotubes. *Environmental Science & Technology*, 2008. **42**: p. 2931–2936.

[6]. Lemus, J., et al., Removal of chlorinated organic volatile compounds by gas phase adsorption with activated carbon. *Chemical Engineering Journal*, 2012. **211-212**: p. 246-254.

[7]. Esteves, I.A.A.C., et al., Adsorption of natural gas and biogas components on activated carbon. S*eparation and Purification Technology*, 2008. **62**(2): p. 281-296.

[8]. Rudkevich, D.M., Emerging supramolecular chemistry of gases. *Angewandte Chemie International Edition*, 2004. **43**(5): p. 558-71.

[9]. Adisa, O.O., B.J. Cox, and J.M. Hill, Encapsulation of methane molecules into carbon nanotubes. *Physica B: Condensed Matter*, 2011. **406**(1): p. 88-93.

[10]. Dincer, I., Technical, environmental and exergetic aspects of hydrogen energy systems. International Journal of Hydrogen Energy, 2002. **27**: p. 265–285.

[11]. Hall, R.C., The nitrogen detector in gas chromatography. *CRC Critical Reviews in Analytical Chemistry*, 1978. **7**(4): p. 323-380.

[12]. Arvanitoyannis, I.S., Modified atmosphere and active packaging technologies, 1st ed.,. CRC Press, USA, 2012.

[13]. McKinlay, A.C., et al., Exceptional behavior over the whole adsorption-storage-delivery cycle for NO in porous metal organic frameworks - drawbacks, Co, Ni-NO. *Journal of the American Chemical Society*, 2008. **130**: p. 10440-10444.

[14]. Wheatley, P.S., et al., NO-releasing zeolites and their antithrombotic properties. *Journal of the American Chemical Society*, 2005. **128**: p. 502-509.

[15]. Mbrlsd, P.J.N., Valve and nozzle construction for aerosol whipped cream dispenser, 1967, Google Patents.

[16]. Hanson, W.H. and R. Smith, Sprayable dispensing system for viscous vegetable oils and apparatus therefore, 1993, Google Patents.

[17]. Zeller, B.L. and D.A. Kim, Gasified food products and methods of preparation thereof. European Patent - EP 2068644B1, 2013.

[18]. Hotchkiss, J.H., B.G. Werner, and E.Y.C. Lee, Addition of carbon dioxide to dairy products to improve quality - a comprehensive review. *Comprehensive Reviews in Food Science and Food Safety*, 2006. **5**: p. 158-168.

[19]. Shomer, R., U. Cogan, and C.H. Mannheim, Thermal death parameters of orange juice and effect of minimal heat treatment and carbon dioxide on shelf-life. *Journal of Food Processing and Preservation*, 1994. **18**(4): p. 305-315.

[20]. Neoh, T.-L., H. Yoshii, and T. Furuta, Encapsulation and release characteristics of carbon dioxide in α-cyclodextrin. *Journal of Inclusion Phenomena and Macrocyclic Chemistry*, 2006. **56**(1-2): p. 125-133.

[21]. Saltveit, M.E., Effect of ethylene on quality of fresh fruits and vegetables. *Postharvest Biology and Technology*, 1999. **15**(3): p. 279-292.

[22]. Khang, N.T., T.H. Binh, and R.D. Bhesh, Application of ehtylene powder for the germination of mung bean sprouts. Poster in 46th Annual AIFST Convention, Bribsbane, Australia, 2013.

[23]. Blankenship, S.M. and J.M. Dole, 1-Methylcyclopropene: a review. *Postharvest Biology and Technology*, 2003. **28**(1): p. 1-25.

[24]. Allan, P.K., A study of metal-organic frameworks for the storage and release of medical gases. Ph.D thesis, University of St. Andrews, UK, 2012 (http://hdl.handle.net/10023/3198).

[25]. Wood, J.P., et al., Adsorption of chlorine dioxide das on activated carbons. *Journal of the Air & Waste Management Association*, 2010. **60**(8): p. 898-906.

[26]. Guzel-Seydim, Z.B., A.K. Greene, and A.C. Seydim, Use of ozone in the food industry. *LWT - Food Science and Technology*, 2004. **37**(4): p. 453-460.

[27]. Springer, B.A., et al., Mechanisms of ligand recognition in myoglobin. *Chemical Reviews*, 1994. **94**: p. 699 - 714.

[28]. Keilin, F.R.S. and J.D. Smith, Haemoglobin and nitrogen fixation in the root nodules of leguminous plants. *Nature*, 1947. **24**: p. 692-695.

[29]. Muller-Dethlefs, K. and P. Hobza, Noncovalent interactions - a challenge for experiment and theory. *Chemical Reviews*, 2000. **100**: p. 143−167.

[30]. Norsko, J., Chemisorption on metal surfaces. *Reports on Progress in Physics*, 1990. **53**(10): p. 1253.

[31]. Masel, R.I., Principles of adsorption and reaction on solid surfaces. 1st ed., Jone Wiley & Sons, Inc, New York, USA, 1996.

[32]. Ishibe, T., et al., Absorption of nitrogen dioxide and nitric oxide by soda lime. *British Journal of Anaesthesia*, 1995. **75**(3): p. 330-333.

[33]. Srivastava, R.K., W. Jozewicz, and C. Singer, SO_2 scrubbing technologies: a review. *Environmental Progress*, 2001. **20**(4): p. 219.

[34]. Keller, J.U. and R. Staudt, Gas adsorption equilibria: experimental methods and adsorptive isotherms. 2005: Springer.

[35]. Sivasankar, B., Engineering chemistry. McGraw-Hill: New York, 2008., 2008.

[36]. Ansón, A., et al., Hydrogen adsorption studies on single wall carbon nanotubes. Carbon, 2004. **42**(7): p. 1243-1248.

[37]. Yoon, J.H. and N.H. Heo, A study on hydrogen encapsulation in $C_{S2.5}$-zeolite A. *The Journal of Physical Chemistry*, 1992. **96**: p. 4997-5000.

[38]. Morris, R.E. and P.S. Wheatley, Gas storage in nanoporous materials. *Angewandte Chemie International Edition*, 2008. **47**(27): p. 4966-81.

[39]. El-Khaiary, M.I., Least-squares regression of adsorption equilibrium data: comparing the options. *Journal of Hazardous Materials*, 2008. **158**(1): p. 73-87.

[40]. Brunauer, S., et al., On a theory of the van der Waals adsorption of gases. *Journal of the American Chemical Society*, 1940. **62**(7): p. 1723-1732.

[41]. Foo, K.Y. and B.H. Hameed, Insights into the modeling of adsorption isotherm systems. *Chemical Engineering Journal*, 2010. **156**(1): p. 2-10.

[42]. Zhou, X., et al., Thermodynamics for the adsorption of SO_2, NO and CO_2 from flue gas on activated carbon fiber. *Chemical Engineering Journal*, 2012. **200-202**: p. 399-404.

[43]. Kumar, K.V., et al., A site energy distribution function from Toth isotherm for adsorption of gases on heterogeneous surfaces. *Physical Chemistry Chemical Physics*, 2011. **13**(13): p. 5753-9.

[44]. Subha, R. and C. Namasivayam, Modeling of adsorption isotherms and kinetics of 2,4,6-trichlorophenol onto microporous $ZnCl_2$ activated coir pith carbon. *Environmental Engineering and Management Journal*, 2008. **18**(4): p. 275-280.

[45]. Fagerlund, G., Determination of specific surface by the BET method. *Materials and Structures*, 1973. **6**(3): p. 239-245.

[46]. Keller, J., R. Staudt, and M. Tomalla, Volume-gravimetric measurements of binary gas adsorption equilibria. *Berichte der Bunsengesellschaft für physikalische Chemie*, 1992. **96**(1): p. 28-32.

[47]. Dreisbach, F., et al., Measurement of adsorption equilibria of pure and mixed corrosive gases: The magnetic suspension balance, in Fundamentals of adsorption, M.D. LeV an, Editor. 1996, Springer US. p. 259-268.

[48]. Keller, J.U., et al., Measurement of gas mixture adsorption equilibria of natural gas compounds on microporous sorbents. *Adsorption*, 1999. **5**(3): p. 199-214.

[49]. Broom, D., Gas sorption measurement techniques, in Hydrogen storage materials. 2011, Springer London. p. 117-139.

[50]. Keller, J., et al. A note on old and new measurement methods for gas adsorption equilibria. in Proceedings of 2nd Pacific Basin conference on adsorption science and technology, Brisbane. 2000.

[51]. Chilev, C., et al., A comparison between the different methods for the measurement of an excess adsorption of pure gases on porous adsorbents at high pressure. *Journal of the University of Chemical Technology and Metallurgy*, 2007. **42**(1): p. 77-84.

[52]. Buss, E., Gravimetric measurement of binary gas adsorption equilibria of methane-carbon dioxide mixtures on activated carbon. *Gas Separation & Purification*, 1995. **9**(3): p. 189-197.

[53]. Alcañiz-Monge, J., et al., Methane storage in activated carbon fibres. *Carbon*, 1996. **35**(2): p. 291-297.

[54]. De Weireld, G., M. Frere, and R. Jadot, Automated determination of high-temperature and high-pressure gas adsorption isotherms using a magnetic suspension balance. *Measurement Science and Technology*, 1999. **10**(2): p. 117.

[55]. Siriwardane, R.V., et al., Adsorption of CO_2 on molecular sieves and activated carbon. Energy & Fuels, 2001. **15**: p. 279-284.

[56]. Belmabkhout, Y., M. Frere, and G. De Weireld, High-pressure adsorption measurements. A comparative study of the volumetric and gravimetric methods. *Measurement Science and Technology*, 2004. **15**(5): p. 848.

[57]. Babaa, M.R., et al., Physical adsorption of carbon tetrachloride on as-produced and on mechanically opened single walled carbon nanotubes. Carbon, 2004. **42**(8-9): p. 1549-1554.

[58]. Rowsell, J.L., et al., Hydrogen sorption in functionalized metal-organic frameworks. Journal of the American Chemical Society, 2004. **126**(18): p. 5666-5667.

[59]. Millward, A.R. and O.M. Yaghi, Metal-organic frameworks with exceptionally high capacity for storage of carbon dioxide at room temperature. Journal of the American Chemical Society, 2005. **127**(51): p. 17998-17999.

[60]. Himeno, S., T. Komatsu, and S. Fujita, High-pressure adsorption equilibria of methane and carbon dioxide on several activated carbons. Journal of Chemical & Engineering Data, 2005. **50**: p. 369-376.

[61]. Lee, J.W., et al., Methane adsorption on multi-walled carbon nanotube at (303.15, 313.15, and 323.15) K. Journal of Chemical & Engineering Data, 2006. **51**: p. 963-967.

[62]. Li, F., et al., Adsorption of carbon dioxide by coconut activated carbon modified with Cu/Ce. Journal of Rare Earths, 2010. **28**: p. 334-337.

[63]. Shang, J., et al., Potassium chabazite - a potential nanocontainer for gas encapsulation. The Journal of Physical Chemistry C, 2010. **114**: p. 22025-22031.

[64]. Keller, J., Theory of measurement of gas-adsorption equilibria by rotational oscillations. Adsorption, 1995. **1**(4): p. 283-290.

[65]. Rave, H., R. Staudt, and J. Keller, Measurement of gas-adsorption equilibria via rotational oscillations. Journal of Thermal Analysis and Calorimetry, 1999. **55**(2): p. 601-608.

[66]. Keller, J.U., H. Rave, and R. Staudt, Measurement of gas absorption in a swelling polymeric material by a combined gravimetric-dynamic method. Macromolecular Chemistry and Physics, 1999. **200**(10): p. 2269-2275.

[67]. Chan, Y.-C. and R.B. Anderson, Temperature-programmed desorption of N_2, Ar, and CO_2 encapsulated in 3A zeolite. Journal of Catalysis, 1977. **50**(2): p. 319-329.

[68]. Chan, Y.C., Encapsulation of gases in zeolite 3A and temperature programmed desorption of the trapped gases. Open Access Dissertations and Theses. Paper 424. McMaster University http://digitalcommons.mcmaster.ca/opendissertations/424, 1977.

[69]. Pinkerton, F., et al., Thermogravimetric measurement of hydrogen absorption in alkali-modified carbon materials. The Journal of Physical Chemistry B, 2000. **104**(40): p. 9460-9467.

[70]. Meisner, G., et al., Enhancing low pressure hydrogen storage in sodium alanates. Journal of Alloys and Compounds, 2002. **337**(1): p. 254-263.

[71]. Majchrzak-Kucęba, I. and W. Nowak, A thermogravimetric study of the adsorption of CO_2 on zeolites synthesized from fly ash. Thermochimica Acta, 2005. **437**(1): p. 67-74.

[72]. Panella, B., M. Hirscher, and B. Ludescher, Low-temperature thermal-desorption mass spectroscopy applied to investigate the hydrogen adsorption on porous materials. Microporous and Mesoporous Materials, 2007. **103**(1): p. 230-234.

[73]. Panella, B., et al., Desorption studies of hydrogen in metal-organic frameworks. Angewandte Chemie International Edition, 2008. **47**(11): p. 2138-2142.

[74]. Channen, E. and R. McIntosh, Investigation of the physically adsorbed state by means of dielectric measurements. Canadian Journal of Chemistry, 1955. **33**(2): p. 172-183.

[75]. Vidal, D., et al., Measurement of physical adsorption of gases at high pressure. Review of scientific instruments, 1990. **61**(4): p. 1314-1318.

[76]. Malbrunot, P., et al., Adsorption measurements of argon, neon, krypton, nitrogen, and methane on activated carbon up to 650 MPa. Langmuir, 1992. **8**(2): p. 577-580.

[77]. Vermesse, J., D. Vidal, and P. Malbrunot, Gas adsorption on zeolites at high pressure. Langmuir 1996. **12**: p. 4190-4196.

[78]. Staudt, R., H. Rave, and J. Keller, Impedance spectroscopic measurements of pure gas adsorption equilibria on zeolites. Adsorption, 1999. **5**(2): p. 159-167.

[79]. Ho, B.T., D.C. Joyce, and B.R. Bhandari, Encapsulation of ethylene gas into alpha-cyclodextrin and characterisation of the inclusion complexes. Food Chemistry, 2011. **127**(2): p. 572-80.

[80]. Ho, B.T., D.C. Joyce, and B.R. Bhandari, Release kinetics of ethylene gas from ethylene-α-cyclodextrin inclusion complexes. Food Chemistry, 2011. **129**(2): p. 259-266.

[81]. Agnihotri, N., et al., Microencapsulation – a novel approach in drug delivery: A review. Indo Global Journal of Pharmaceutical Sciences, 2012. **2**(1): p. 1-20.

[82]. Zhang, P., H. Wanko, and J. Ulrich, Adsorption of SO_2 on activated carbon for low gas concentrations. Chemical Engineering & Technology, 2007. **30**(5): p. 635-641.

[83]. Thommes, M., Physical adsorption characterization of nanoporous materials. Chemie Ingenieur Technik, 2010. **82**(7): p. 1059-1073.

[84]. Sircar, S., C. Golden, and B. Rao, Activated carbon for gas separation and storage. Carbon, 1996. **34**(1): p. 1-12.

[85]. Demiral, H., et al., Production of activated carbon from olive bagasse by physical activation. Chemical Engineering Research and Design, 2011. **89**(2): p. 206-213.

[86]. Oubagaranadin, J.U.K. and Z.V.P. Murthy, Activated carbons: classifications, properties and applications (pp. 239-266), chapter 6: In Kwiatkowski, James F. (Ed.), Activated carbon: classifications, properties and applications, Nova Science Publishers Inc, USA. 2011.

[87]. Incorporated, C.C., Activated carbon - manufacture, structure & properties. Activated Carbon & Related Technology, USA, 2006.

[88]. Matranga, K.R., R.L. Myers, and E.D. Glandt, Storage of natural gas by adsorption on activated carbon. Chemical Engineering Science, 1992. **47**(7): p. 1569-1579.

[89]. Wu, J., Modeling adsorption of organic compounds on activated carbon: a multivariate approach. Ph.D thesis, Institut de chimie - Université de Neuchâtel, Sweden, 2004.

[90]. Pevida, C., et al., Surface modification of activated carbons for CO_2 capture. Applied Surface Science, 2008. **254**(22): p. 7165-7172.

[91]. Wickramaratne, N.P. and M. Jaroniec, Activated carbon spheres for CO_2 adsorption. ACS Applied Materials & Interfaces, 2013. **5**(5): p. 1849-55.

[92]. Hotton, A.J., J.T. Barminas, and S.A. Osemeahon, Studies on the adsorption efficiency of activated carbon for pesticide vapour. African Journal of Pure and Applied Chemistry, 2011. **5**(14): p. 466-473.

[93]. Yoon, J.H. and M.W. Huh, Encapsulation of simple gases in zeolites. The Journal of Physical Chemistry, 1994. **98**: p. 3202-06.

[94]. Przepiórski, J., M. Skrodzewicz, and A.W. Morawski, High temperature ammonia treatment of activated carbon for enhancement of CO_2 adsorption. Applied Surface Science, 2004. **225**(1-4): p. 235-242.

[95]. Figueiredo, J.L., et al., Modification of the surface chemistry of activated carbons. Carbon, 1999. **37**: p. 1379-89.

[96]. Zhang, Z., et al., Enhancement of CO_2 adsorption on high surface area activated carbon modified by N2, H2 and ammonia. Chemical Engineering Journal, 2010. **160**(2): p. 571-577.

[97]. Caglayan, B.S. and A.E. Aksoylu, CO_2 adsorption on chemically modified activated carbon. Journal of Hazardous Materials, 2013. **252-253**: p. 19-28.

[98]. Shafeeyan, M.S., et al., A review on surface modification of activated carbon for carbon dioxide adsorption. Journal of Analytical and Applied Pyrolysis, 2010. **89**(2): p. 143-151.

[99]. Mangun, C.L., J.A. DeBarr, and J. Economy, Adsorption of sulfur dioxide on ammonia-treated activated carbon fiber. Carbon, 2001. **39**: p. 1689–1696.

[100]. Prauchner, M.J. and F. Rodríguez-Reinoso, Preparation of granular activated carbons for adsorption of natural gas. Microporous and Mesoporous Materials, 2008. **109**(1-3): p. 581-584.

[101]. Radosz, M., et al., Flue-gas carbon capture on carbonaceous sorbents toward a low-cost multifunctional carbon filter for "green" energy producers. Industrial & Engineering Chemistry Research, 2008. **47**: p. 3783-3794.

[102]. Matranga, K.R., A.L. Myers, and E.D. Glandt, Storage of natural gas by adsorption on activated carbon. Chemical Engineering Science, 1992. **47**(7): p. 1569-1579.

[103]. Vargas, D.P., et al., CO2 adsorption on binderless activated carbon monoliths. Adsorption, 2010. **17**(3): p. 497-504.

[104]. Chien, H.W., W.B. Tsai, and S. Jiang, Direct cell encapsulation in biodegradable and functionalizable carboxybetaine hydrogels. Biomaterials, 2012. **33**(23): p. 5706-12.

[105]. Yu, C.-H., A review of CO_2 capture by absorption and adsorption. Aerosol and Air Quality Research, 2012.

[106]. Grande, C.A., Advances in pressure swing adsorption for gas separation. ISRN Chemical Engineering, 2012. **2012**: p. 1-13.

[107]. An, H. and B. Feng, Desorption of CO_2 from activated carbon fibre-phenolic resin composite by electrothermal effect. International Journal of Greenhouse Gas Control, 2010. **4**(1): p. 57-63.

[108]. Gray, P. and D. Do, Adsorption and desorption of gaseous sorbates on a bidispersed particle with Freundlich isotherm: I. Theoretical analysis. Gas Separation & Purification, 1989. **3**(4): p. 193-200.

[109]. Gray, P. and D. Do, Adsorption and desorption of gaseous sorbates on a bidispersed particle with Freundlich isotherm: II. Experimental study of sulphur dioxide sorption on activated carbon particles. Gas Separation & Purification, 1989. **3**(4): p. 201-208.

[110]. Sabio, E., et al., Thermal regeneration of activated carbon saturated with p-nitrophenol. Carbon, 2004. **42**(11): p. 2285-2293.

[111]. Sanmiguel, G., S.D. Lambert, and N.J.D. Graham, The regeneration of field-spent granular activated carbons. Water Research, 2001. **35**(11): p. 2740–2748.

[112]. Narbaitz, R.M. and A. Karimi-Jashni, Electrochemical regeneration of granular activated carbons loaded with phenol and natural organic matter. Environmental Technology, 2009. **30**(1): p. 27-36.

[113]. Shende, R.V. and V.V. Mahajani, Wet oxidative regeneration of activated carbon loaded with reactive dye. Waste Management, 2002. **22**: p. 73–83.

[114]. Martin, R.J. and N. Wj, The repeated exhaustion and chemical regeneration of activated carbon. Water Research, 1987. **21**(8): p. 961-965.

[115]. Lim, J.L. and M. Okada, Regeneration of granular activated carbon using ultrasound. Ultrasonics Sonochemistry, 2005. **12**(4): p. 277-82.

[116]. Salvadoor, F. and C.S. Jimbnez, A new method for regenerating activated carbon by thermal desorption with liquid water under subcritical conditions. Carbon 1995. **34**(4): p. 511-516.

[117]. Nakano, Y., et al., Biodegradation of trichloroethylene (TCE) adsorbed on granular activated carbon (GAC). Wat.Res., 2000. **34**(17): p. 4139-4142.

[118]. Iijima, S., Helical microtubules of graphitic carbon. Nature, 1991. **354**: p. 56-58.

[119]. Darkrima, F.L., P. Malbrunota, and G.P. Tartagliab, Review of hydrogen storage by adsorption in carbon nanotubes. International Journal of Hydrogen Energy, 2002. **27**: p. 93-202.

[120]. Bonard, J.M., et al., Physics and chemistry of carbon nanostructures. European Chemistry Chronicle, 1998. **3**: p. 9-16.

[121]. Fujiwaraa, A., et al., Gas adsorption in the inside and outside of single-walled carbon nanotubes. Chemical Physics Letters, 2001. **336**: p. 205-211.

[122]. Levesque, D., et al., Monte carlo simulations of hydrogen storage in carbon nanotubes. Journal of Physics: Condensed Matter, 2002. **14**: p. 9285–9293.

[123]. Elerskii, A.V., Carbon nanotubes. Physics-Uspekhi 1997. **40**(9): p. 899-924.

[124]. Elerskii, A.V., Sorption properties of carbon nanostructures. Physics-Uspekhi 2004. **47**(11): p. 1119-1154.

[125]. Oddy, S., J. Poupore, and F.H. Tezel, Separation of CO_2 and CH_4 on CaX zeolite for use in landfill gas separation. The Canadian Journal of Chemical Engineering, 2013. **91**(6): p. 1031-1039.

[126]. Zhao, J., et al., Gas molecule adsorption in carbon nanotubes and nanotube bundles. Nanotechnology 2002. **13**: p. 195-200.

[127]. Shi, W. and J. Johnson, Gas adsorption on heterogeneous single-walled carbon nanotube bundles. Physical Review Letters, 2003. **91**(1).

[128]. Muris, M., et al., Methane and krypton adsorption on single-Wwalled carbon nanotubes. Langmuir, 2000. **16**: p. 7019-7022.

[129]. Furmaniak, S., et al., Simulation of SF_6 adsorption on the bundles of single walled carbon nanotubes. Microporous and Mesoporous Materials, 2012. **154**: p. 51-55.

[130]. Reyes-Reyes, M., et al., Efficient encapsulation of gaseous nitrogen inside carbon nanotubes with bamboo-like structure using aerosol thermolysis. Chemical Physics Letters, 2004. **396**(1-3): p. 167-173.

[131]. Su, F., et al., Capture of CO_2 from flue gas via multiwalled carbon nanotubes. Science of the Total Environment, 2009. **407**(8): p. 3017-23.

[132]. Li, X., Y. Fan, and F. Watari, Current investigations into carbon nanotubes for biomedical application. Biomedical Materials, 2010. **5**(2): p. 22001.

[133]. Vela, S. and F. Huarte-Larrañaga, A molecular dynamics simulation of methane adsorption in single walled carbon nanotube bundles. Carbon, 2011. **49**(13): p. 4544-4553.

[134]. Barberio, M., et al., Oxygen interaction with single-walled carbon nanotubes. Superlattices and Microstructures, 2009. **46**(1-2): p. 365-368.

[135]. Wu, X.B., et al., Hydrogen uptake by carbon nanotubes. Internaional journal of Hydrogen Energy, 2000. **25**(261-265).

[136]. Liu, C., et al., Hydrogen storage in single-walled carbon nanotubes at room temperature. Science, 1999. **286**: p. 1127-29.

[137]. Yang, R.T., Hydrogen storage by alkali-doped carbon nanotubes-revisited. Carbon, 2000. **38**: p. 623–641.

[138]. Ye, Y., et al., Hydrogen adsorption and cohesive energy of single-walled carbon nanotubes. Applied Physics Letters, 1999. **74**(16): p. 2307.

[139]. Wang, Q. and J.K. Johnson, Molecular simulation of hydrogen adsorption in single-walled carbon nanotubes and idealized carbon slit pores. The Journal of Chemical Physics, 1999. **110**(1): p. 577.

[140]. Yin, Y.F., T. Mays, and B. McEnaney, Molecular simulations of hydrogen storage in carbon nanotube arrays. Langmuir, 2000. **16**: p. 10521-10527.

[141]. Chen, P., High H2 uptake by alkali-doped carbon nanotubes under ambient pressure and moderate temperatures. Science, 1999. **285**(5424): p. 91-93.

[142]. Cinke, M., et al., CO_2 adsorption in single-walled carbon nanotubes. Chemical Physics Letters, 2003. **376**(5-6): p. 761-766.

[143]. Hsu, S.-C., et al., Thermodynamics and regeneration studies of CO2 adsorption on multiwalled carbon nanotubes. Chemical Engineering Science, 2010. **65**(4): p. 1354-1361.

[144]. Ulbricht, H., et al., Desorption kinetics and interaction of Xe with single-wall carbon nanotube bundles. Chemical Physics Letters, 2002. **363**(3–4): p. 252-260.

[145]. Lee, H., et al., Hydrogen desorption properties of multiwall carbon nanotubes with closed and open structures. Applied Physics Letters, 2002. **80**(4): p. 577.

[146]. Kim, H.-S., et al., Hydrogen storage in Ni nanoparticle-dispersed multiwalled carbon nanotubes. The Journal of Physical Chemistry B, 2005. **109**(18): p. 8983-8986.

[147]. Lee, J.W., et al., Hydrogen storage and desorption properties of Ni-dispersed carbon nanotubes. Applied Physics Letters, 2006. **88**(14): p. 143126.

[148]. Bienfait, M. and J.A. Venables, Kinetics of adsorption and desorption using Auger electron spectroscopy: Application to xenon covered (0001) graphite. Surface Science, 1977. **64**(2): p. 425-436.

[149]. Carlos Ruiz-Suarez, J., et al., Zero-order desorption of Xe from (0001) graphite: an experimental study and a theoretical model. Surface Science, 1991. **243**(1–3): p. 219-226.

[150]. Hardie, S.M.L., et al., Carbon dioxide capture using a zeolite molecular sieve sampling system for isotopic studies (^{13}C and ^{14}C) of respiration. Radiocarbon, 2005. **47**(3): p. 441-451.

[151]. Lobo, R.F., Introduction to the structural chemistry of zeolites. in Handbook of zeolite science and technology, edited by Auerbach, et al. (2003), New York: USA, 2003.

[152]. Armbruster, T. and M.E. Gunter, Crystal structures of natural zeolites. The Mineralogical Society Of America, 2001. **45**(1): p. 1-67.

[153]. Georgiev, D., et al., Synthetic zeolites - structure, classification, current trends in zeolite synthesis - review. 4th - 5th International Science conference in Stara Zagora, Bulgaria 2009.

[154]. Baerlocher, C. and L.B. McCusker, Database of zeolite structures: http://www.iza-structure.org/databases/. Accessed by 10 September 2013. 2010.

[155]. First, E.L., et al., ZEOMICS: zeolites and microporous structures characterization. http://helios.princeton.edu/zeomics/. Accessed by 12 September 2013. 2011.

[156]. Gesser, H.D., et al., Pressure dependence of methane encapsulation in type 3A zeolites. Zeolites, 1983. **4**: p. 22-24.

[157]. Matsuoka, S., et al., Stability of krypton fixed in zeolite-3A and -5A. Journal of Nuclear Science and Technology, 1986. **23**(1): p. 29-36.

[158]. Kalinnikova, I.A.M., N.N.; Nikiforov, V.S.; Pribylov, A.A.; Serpinskii, V.V.; Tishin, I.V., Encapsulation of oxygen and nitrogen by zeolites for their storage. Chemical and Petroleum Engineering, 1986: p. 271-273.

[159]. Itabashi, K., T. Takaishi, and T. Ohgushi, Encapsulation of krypton with (K, MII) - A zeolites. Bulletin of the Chemical Society of Japan, 1943. **54**: p. 1943-45.

[160]. Graham, P., A.D. Hughes, and L.V.C. Rees, Sorption of binary gas mixtures in zeolites - Sorption of nitrogen and carbon dioxide mixtures in silicalite Gas Separation & Purification, 1988. **3**.

[161]. Golden, T.C. and S. Sircar, Synthetic heterogeneity in X zeolite for gas adsorption. Journal of Colloid and Interface Science, 1991. **147**(1).

[162]. Yoon, J.H., Pressure-dependent hydrogen encapsulation in Na_{12}-zeolite A. The Journal of Physical Chemistry, 1992. **97**: p. 6066-6068.

[163]. Heo, N.H., W.T. Taik Lim, and K. Seff, Crystal structures of encapsulates within zeolites. 2. Argon in zeolite A. The Journal of Physical Chemistry, 1996. **100**: p. 13725-13731.

[164]. Heo, N.H., K.H. Cho, and J.T. Kim, Crystal structures of encapsulates within zeolites. 1. krypton in zeolite The Journal of Physical Chemistry, 1994. **98**: p. 13328-13333.

[165]. Cavenati, S., C.A. Grande, and A.E. Rodrigues, Adsorption equilibrium of methane, carbon dioxide, and nitrogen on zeolite 13X at high pressures. Journal of Chemical and Engineering Data, 2004. **49**(4): p. 1095-1101.

[166]. Singh, R.K. and P. Webley, Adsorption of N_2, O_2, and Ar in potassium chabazite. Adsorption, 2005. **11**: p. 173–177.

[167]. Hayashi, H., et al., Zeolite A imidazolate frameworks. Nature Materials, 2007. **6**(7): p. 501-6.

[168]. Vitillo, J.G., et al., Theoretical maximal storage of hydrogen in zeolitic frameworks. Physical Chemistry Chemical Physics, 2005. **7**(23): p. 3948.

[169]. Weitkamp, J., M. Fritz, and S. Ernst, Zeolites as media for hydrogen storage. International Journal of Hydrogen Energy, 1995. **20**(12): p. 967 970.

[170]. Pavelic, K. and M. Hadzija, Medical applications of zeolites, chapter 24: In Handbook of zeolite science and technology. New York: Dekker: 1143-1174. 2003.

[171]. Mumpton, F.A., La roca magica: Uses of natural zeolites in agriculture and industry. Proceedings of the National Academy of Sciences, 1999. **96**(7): p. 3463-3470.

[172]. Thomas, J. and B. Ballantyne, Toxicological assessment of zeolites. International Journal of Toxicology, 1992. **11**(3): p. 259-273.

[173]. Xiao, B., et al., High-capacity hydrogen and nitric oxide adsorption and storage in a metal-organic framework. Journal of the American Chemical Society, 2007. **129**(1203-1209).

[174]. Dat, A., Applications of mesoporous silica and zeolites for drug delivery. Ph.D thesis, University of Iowa. http://ir.uiowa.edu/etd/3442., 2012.

[175]. Wang, D., et al., Controlled release and conversion of guest species in zeolite microcapsules. New Journal of Chemistry, 2005. **29**(2): p. 272.

[176]. Hoskins, B.F. and R. Robson, Infinite polymeric frameworks consisting of three dimensionally linked rod-like segments. Journal of the American Chemical Society, 1989. **111**(15): p. 5964-5965.

[177]. Britt, D., D. Tranchemontagne, and O.M. Yaghi, Metal-organic frameworks with high capacity and selectivity for harmful gases. Proceedings of the National Academy of Sciences of the United States of America, 2008. **105**(33): p. 11623-7.

[178]. Ma, S., Gas adsorption applications of porous metal–organic frameworks. Pure and Applied Chemistry, 2009. **81**(12): p. 2235-2251.

[179]. Furukawa, H., et al., Ultrahigh porosity in metal-organic frameworks. Science, 2010. **329**(5990): p. 424-8.

[180]. Rowsell, J.L., et al., Gas adsorption sites in a large-pore metal-organic framework. Science, 2005. **309**(5739): p. 1350-4.

[181]. Horcajada, P., et al., Metal-organic frameworks in biomedicine. Chemical Reviews, 2012. **112**(2): p. 1232-68.

[182]. James, S.L., Metal-organic frameworks. Chemical Society Reviews, 2003. **32**(5): p. 276.

[183]. Tranchemontagne, D.J., J.R. Hunt, and O.M. Yaghi, Room temperature synthesis of metal-organic frameworks: MOF-5, MOF-74, MOF-177, MOF-199, and IRMOF-0. Tetrahedron, 2008. **64**(36): p. 8553-8557.

[184]. Almeida Paz, F.A. and J. Klinowski, Hydrothermal synthesis and structural characterization of a novel cadmium-organic framework. Journal of Solid State Chemistry, 2004. **177**(10): p. 3423-3432.

[185]. Clausen, H.F., et al., Solvothermal synthesis of new metal organic framework structures in the zinc–terephthalic acid-dimethyl formamide system. Journal of Solid State Chemistry, 2005. **178**(11): p. 3342-3351.

[186]. Klinowski, J., et al., Microwave-assisted synthesis of metal-organic frameworks. Dalton Trans, 2011. **40**(2): p. 321-30.

[187]. MacGillivray, L.R., et al., Supramolecular control of reactivity in the solid state: from templates to ladderanes to metal−organic frameworks. Accounts of Chemical Research, 2008. **41**(2): p. 280-291.

[188]. Bae, Y.-S., et al., Enhancement of CO_2/N_2 selectivity in a metal-organic framework by cavity modification. Journal of Materials Chemistry, 2009. **19**(15): p. 2131.

[189]. Lin, Y., et al., Polyethyleneimine incorporated metal-organic frameworks adsorbent for highly selective CO_2 capture. Scientific Reports, 2013. **3**: p. 1859.

[190]. Si, X., et al., Adjustable structure transition and improved gases (H_2, CO_2) adsorption property of metal-organic framework MIL-53 by encapsulation of BNHx. Dalton Trans, 2012. **41**(11): p. 3119-22.

[191]. Volkringer, C. and S.M. Cohen, Generating reactive MILs: isocyanate- and isothiocyanate-bearing MILs through postsynthetic modification. Angewandte Chemie International Edition, 2010. **49**(27): p. 4644-8.

[192]. Xu, Q., et al., Li-modified metal–organic frameworks for CO_2/CH_4 separation: a route to achieving high adsorption selectivity. Journal of Materials Chemistry, 2010. **20**(4): p. 706.

[193]. Hinks, N.J., et al., Metal organic frameworks as NO delivery materials for biological applications. Microporous and Mesoporous Materials, 2010. **129**(3): p. 330-334.

[194]. Dietzel, P.D., et al., Adsorption properties and structure of CO_2 adsorbed on open coordination sites of metal-organic framework Ni_2(dhtp) from gas adsorption, IR spectroscopy and X-ray diffraction. Chemical communications (Cambridge, England), 2008(41): p. 5125-7.

[195]. Britt, D., et al., Highly efficient separation of carbon dioxide by a metal-organic framework replete with open metal sites. Proceedings of the National Academy of Sciences of the United States of America, 2009. **106**(49): p. 20637-40.

[196]. Chen, B., et al., Cu2(ATC),6H2O: Design of open metal sites in porous metal-organic crystals (ATC: 1,3,5,7-Adamantane Tetracarboxylate). Journal of the American Chemical Society, 2000. **122**: p. 11559-11560.

[197]. Ma, S. and H.C. Zhou, Gas storage in porous metal-organic frameworks for clean energy applications. Chemical communications (Cambridge, England), 2010. **46**(1): p. 44-53.

[198]. Li, J.-R., et al., Carbon dioxide capture-related gas adsorption and separation in metal-organic frameworks. Coordination Chemistry Reviews, 2011. **255**(15-16): p. 1791-1823.

[199]. Lee, J., J. Li, and J. Jagiello, Gas sorption properties of microporous metal organic frameworks. Journal of Solid State Chemistry, 2005. **178**(8): p. 2527-2532.

[200]. Yazaydın, A.O., et al., Screening of metal-organic frameworks for carbon dioxide capture. Journal of the American Chemical Society, 2009. **131**: p. 18198–18199.

[201]. Nijem, N., et al., Interaction of molecular hydrogen with microporous metal organic framework materials at room temperature. J. AM. CHEM. SOC, 2010. **132**(50): p. 1654-1664.

[202]. Dietzel, P.D., et al., Interaction of hydrogen with accessible metal sites in the metal-organic frameworks M(2)(dhtp) (CPO-27-M; M = Ni, Co, Mg). Chemical communications (Cambridge, England), 2010. **46**(27): p. 4962-4.

[203]. Vaidhyanathan, R., et al., Direct observation and quantification of CO2 binding within an amine-functionalized nanoporous solid. Science, 2010. **330**(6004): p. 650-3.

[204]. Eddaoudi, M., et al., Systematic design of pore size and functionality in isoreticular MOFs and their application in methane storage. Science, 2002. **295**(5554): p. 469-72.

[205]. Gassensmith, J.J., et al., Strong and reversible binding of carbon dioxide in a green metal-organic framework. Journal of the American Chemical Society, 2011. **133**(39): p. 15312-5.

[206]. Saha, D., et al., A magnesium-based multifunctional metal-organic framework: synthesis, thermally induced structural variation, selective gas adsorption, photoluminescence and heterogeneous catalytic study. Dalton Trans, 2013.

[207]. Li, Y. and R.T. Yang, Gas adsorption and storage in metal-organic framework MOF-177. Langmuir, 2007. **23**: p. 12937-12944.

[208]. Wong-Foy, A.G., A.J. Matzger, and O.M. Yaghi, Exceptional H_2 saturation uptake in microporous metal-organic frameworks. Journal of the American Chemical Society, 2006. **128**: p. 3494-3495.

[209]. Pan, J., et al., The 3D porous metal–organic frameworks based on bis(pyrazinyl)–trizole: structures, photoluminescence and gas adsorption properties. CrystEngComm, 2013. **15**(28): p. 5673.

[210]. Hamon, L., et al., Comparative study of hydrogen sulfide adsorption in the MIL-53(Al, Cr, Fe), MIL-47(V), MIL-100(Cr), and MIL-101(Cr) metal-organic frameworks at room temperature. Journal of the American Chemical Society, 2009. **131**: p. 8775–8777.

[211]. Allan, P.K., et al., Metal-organic frameworks for the storage and delivery of biologically active hydrogen sulfide. Dalton Trans, 2012. **41**(14): p. 4060-4066.

[212]. Petit, C., B. Mendoza, and T.J. Bandosz, Reactive adsorption of ammonia on Cu-based MOF/graphene composites. Langmuir, 2010. **26**(19): p. 15302-9.

[213]. Cramer, F. and F.M. Henglein, Einschlußverbindungen der cyclodextrine mit gasen. Angewandte Chemie International Edition, 1956. **68**(20): p. 649-649.

[214]. Szejtli, J., Downstream processing using cyclodextrins. Trend in Biotechnology, 1989. **7**(7): p. 170-174.

[215]. Bersier, P.M., J. Bersier, and B. Klingert, Electrochemistry of cyclodextrins and cyclodextrin complexes. Elechwanalysis, 1991. **3**: p. 443-455.

[216]. Connors, K.A., The stability of cyclodextrin complexes in solution. Chemical Reviews, 1997. **97**(5): p. 1325-1358.

[217]. Del Valle, E.M.M., Cyclodextrins and their uses: a review. Process Biochemistry, 2004. **39**(9): p. 1033-1046.

[218]. Astray, G., et al., A review on the use of cyclodextrins in foods. Food Hydrocolloids, 2009. **23**(7): p. 1631-1640.

[219]. Rawat, S. and S.K. Jain, Solubility enhancement of celecoxib using beta-cyclodextrin inclusion complexes. European Journal of Pharmaceutics and Biopharmaceutics, 2004. **57**(2): p. 263-7.

[220]. Irie, T. and K. Uekama, Pharmaceutical applications of cyclodextrins. III. Toxicological issues and safety evaluation. Journal of Pharmaceutical Sciences, 1997. **86**: p. 147-162.

[221]. Loftsson, T. and D. Duchene, Cyclodextrins and their pharmaceutical applications. International Journal of Pharmaceutics, 2007. **329**(1-2): p. 1-11.

[222]. Hedges, A.R., Industrial applications of cyclodextrins. Chemical Reviews, 1998. **98**(5): p. 2035-2044.

[223]. Szente, L. and J. Szejtli, Cyclodextrins as food ingredients. Trends in Food Science & Technology, 2004. **15**(3-4): p. 137-142.

[224]. Singh, M., R. Sharma, and U.C. Banerjee, Biotechnological applications of cyclodextrins. Biotechnology Advances, 2002. **20**: p. 341–359.

[225]. Neoh, T.L., et al., Kinetics of molecular encapsulation of 1-methylcyclopropene into alpha-cyclodextrin. Journal of Agricultural and Food Chemistry, 2007. **55**: p. 11020-11026.

[226]. Trotta, F., et al., Cyclodextrin nanosponges as effective gas carriers. Journal of Inclusion Phenomena and Macrocyclic Chemistry, 2011. **71**(1-2): p. 189-194.

[227]. Szejtli, J., Cyclodextrin inclusion complexes, in Cyclodextrin technology. 1988, Springer Netherlands. p. 79-185.

[228]. Hedges, A.R., W.J. Shieh, and C.T. Sikorski, Use of cyclodextrins for encapsulation in the use and treatment of food products. In Encapsulation and controlled release of food ingredients; Risch, S., et al.; ACS Symposium Series; American Chemical Society: Washington, DC. 1995. **590**: p. 60-71.

[229]. Dubois, L., et al., Dynamics of xenon inside hydrophobic cavities as probed by NMR relaxation of dissolved laser-polarised xenon. Journal of Physical Chemistry B, 2004. **108**(2): p. 767-773.

[230]. Bartik, K., et al., Probing molecular cavities in α-cyclodextrin solutions by xenon NMR. Journal of Magnetic Resonance, Series B, 1995. **109**(2): p. 164-168.

[231]. Trotta, F., M. Zanetti, and R. Cavalli, Cyclodextrin-based nanosponges as drug carriers. Beilstein Journal of Organic Chemistry, 2012. **8**: p. 2091-9.

[232]. Cavalli, R., et al., Nanosponge formulations as oxygen delivery systems. International Journal of Pharmaceutics, 2010. **402**(1-2): p. 254-7.

[233]. 233. Schneiderman, E. and A.M. Stalcup, Cyclodextrins - a versatile tool in separation science. Journal of Chromatography B, 2000. **745**: p. 83–102.

[234]. 234. Liu, L. and Q.-X. Guo, The driving forces in the inclusion complexation of cyclodextrins. Journal of Inclusion Phenomena and Macrocyclic Chemistry, 2002. **42**(1-2): p. 1-14.

[235]. Saenger, W., Crystal packing patterns of cyclodextrin inclusion complexes. in Clathrate compounds, molecular inclusion phenomena, and cyclodextrins advances in inclusion science. Edited by Atwood et al. (1984). Proceedings of the third international symposium on clathrate compounds and molecular inclusion phenomena and the second international symposium on cyclodextrins, Tokyo, Japan, 1985. **3**: p. 445-454.

[236]. He, Y., et al., Cyclodextrin-based aggregates and characterization by microscopy. Micron, 2008. **39**(5): p. 495-516.

[237]. Saenger, W., et al., Structures of the common cyclodextrins and their larger analoguess beyond the doughnut. Chemical Reviews 1998. **98**: p. 1787−1802.

[238]. Avrami, M., Kinetics of phase change. II Transformation-time relations for random distribution of nuclei. The Journal of Chemical Physics, 1940. **8**(2): p. 212.

[239]. Das, R.K., N. Kasoju, and U. Bora, Encapsulation of curcumin in alginate-chitosan-pluronic composite nanoparticles for delivery to cancer cells. Nanomedicine, 2010. **6**(1): p. 153-60.

[240]. Klingspor, J., et al., Similarities between lime and limestone in wet-dry scrubbing. Chemical Engineering and Processing: Process Intensification, 1984. **18**(5): p. 239-247.

[241]. Atwood, J.L., L.J. Barbour, and A. Jerga, Storage of methane and freon by interstitial van der waals confinement. Science, 2002. **296**(5577): p. 2367-2369.

[242]. Atwood, J.L., L.J. Barbour, and A. Jerga, A new type of material for the recovery of hydrogen from gas mixtures. Angew Chem Int Ed Engl, 2004. **43**(22): p. 2948-50.

[243]. Cram, D.J., et al., Shell closure of two cavitands forms carcerand complexes with components of the medium as permanent guests. J Am Chem Soc, 1985. **107**(8): p. 2575-2576.

[244]. Warmuth, R. and J. Yoon, Recent highlights in hemicarcerand chemistry. Accounts of Chemical Research, 2001. **34**(2): p. 95-105.

[245]. Bartik, K., et al., ^{129}Xe and ^{1}H NMR study of the reversible trapping of xenon by cryptophane-a in organic solution. Journal of the American Chemical Society, 1998. **120**(4): p. 784-791.

[246]. Leontiev, A.V., A.W. Saleh, and D.M. Rudkevich, Hydrophobic encapsulation of hydrocarbon gases. Organic Letters, 2007. **9**(9): p. 1753-1755.

[247]. Branda, N., et al., Control of self-assembly and reversible encapsulation of xenon in a self-assembling dimer by acid-base chemistry. J Am Chem Soc, 1995. **117**(1): p. 85-88.

[248]. Leontiev, A.V. and D.M. Rudkevich, Encapsulation of gases in the solid state. Chemical communications (Cambridge, England), 2004(13): p. 1468-9.

[249]. Louis, S. and Z. Andreas, Hydrogen-storage materials for mobile applications. Nature, 2001. **414**(6861): p. 353-358.

[250]. Energy Efficiency & Renewable Energy (EERE), Hydrogen storage. U.S Department of Energy, http://energy.gov/eere/office-energy-efficiency-renewable-energy. Accessed by 10 September 2013., (2013).

[251]. Rao, A.M., et al., Evidence for charge transfer in doped carbon nanotube bundles from Raman scattering. Nature, 1997. **338**: p. 257-259.

[252]. Jhi, S.H., S.G. Louie, and M.L. Cohen, Electronic properties of oxidized carbon nanotubes. Physical Review Letters, 2000. **85**(8): p. 1710 - 1713.

[253]. Kong, J., Nanotube molecular wires as chemical sensors. Science, 2000. **287**(5453): p. 622-625.

[254]. Lee, R.S., et al., Conductivity enhancement in single-walled carbon nanotube bundles doped with K and Br. Nature, 1997. **388**: p. 255-257.

[255]. Adu, C.K.W., et al., Carbon nanotubes: a thermoelectric nano nose. Chemical Physics Letters, 2001. **337**(1-3): p. 31-35.

[256]. Sumanasekera, G.U., et al., Effects of gas adsorption and collisions on electrical transport. Physics Review Letters, 2000. **85**(5): p. 1096-1099.

[257]. Tans, S.J., A.R.M. Verschueren, and C. Dekker, Room-temperature transistor based on a single carbon nanotube. Nature, 1998. **393**.

[258]. Martel, R., et al., Single- and multi-wall carbon nanotube field-effect transistors. Applied Physics Letters, 1998. **73**(17): p. 2447.

[259]. Collins, P.G., et al., Extreme oxygen sensitivity of electronic properties of carbon nanotubes. Science, 2000. **287**(5459): p. 1801-1804.

[260]. Trowell, O.A., Effects of carbon dioxide in the heart and circulation. Nature, 1944. **153**: p. 686.

[261]. Lowicka, E. and J. Betowski, Hydrogen sulfide (H2S) - the third gas of interest for pharmacologists. Pharmacological Reports, 2007. **59**: p. 4-24.

[262]. Keefer, L.K., Biomaterials: Thwarting thrombus. Nature Materials, 2003. **2**(6): p. 357-358.

[263]. Dietzel, P.D., et al., Structural changes and coordinatively unsaturated metal atoms on dehydration of honeycomb analogous microporous metal-organic frameworks. Chemistry, 2008. **14**(8): p. 2389-97.

[264]. Dubey, R.S., T.C.; Rao, K.U.B., Microencapsulation technology and applications. Defence Science Journal, 2009. **59**(1): p. 82-95.

[265]. Bermas, E.M., Refrigerator freshener. United States Patent. Patent Number - 5,468,447, 1995.

[266]. McGowan, K.F., Odor adsorptive filter for refrigerators and freezers. United States Patent. Patent No - US 6,346,143 B1, 2002.

[267]. Nedovica, V., et al., An overview of encapsulation technologies for food applications. Procedia Food Science, 2011. **1**: p. 1806 -15.

[268]. Bisperillk, C., et al., Foaming ingredient and powders containg it. United States Patent. Patent N0 - US 6,713,113 B2, 2004.

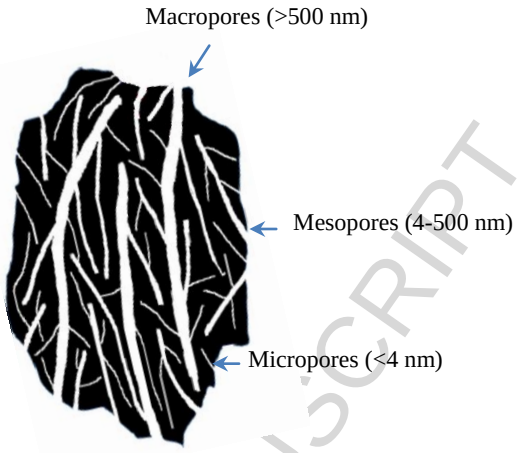

Fig 1: Schematic representation of three types of pores in an activated carbon particle (Adapted from [89])

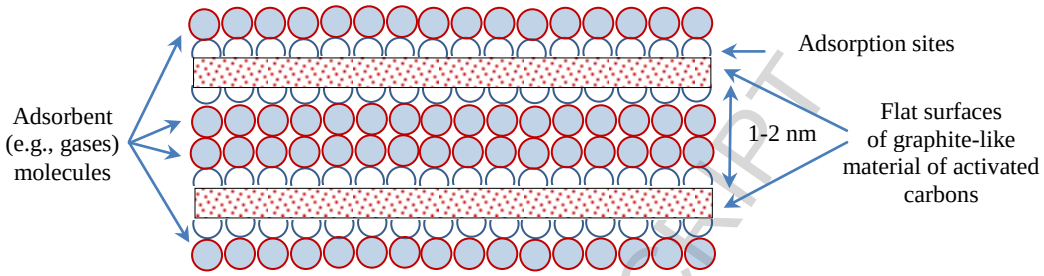

Fig 2: The model of activate carbon with two intercalated layers of gases between single planes of graphite (Adapted from [88])

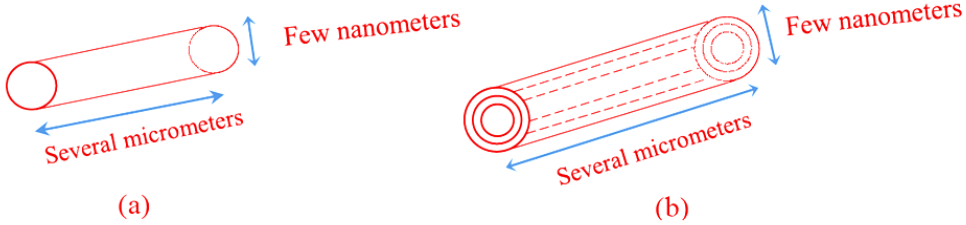

Fig 3: Illustration of single-walled (a) and multi-walled (b) carbon nanotubes

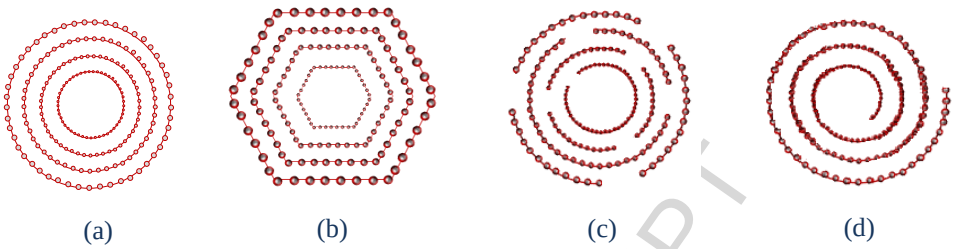

Fig 4: Illustration of various possible arrangements of multi-walled carbon nanotubes (a): Russian doll; (b): hexahedral prisms; (c): papier-mache; and (d): scroll [123]

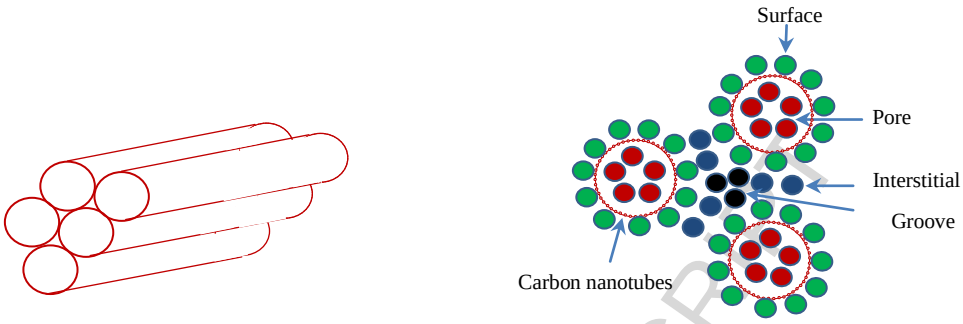

(a) (b)

Fig 5: A bundle of nanotubes (a) and various possible adsorption sites of a tube bundle (b)

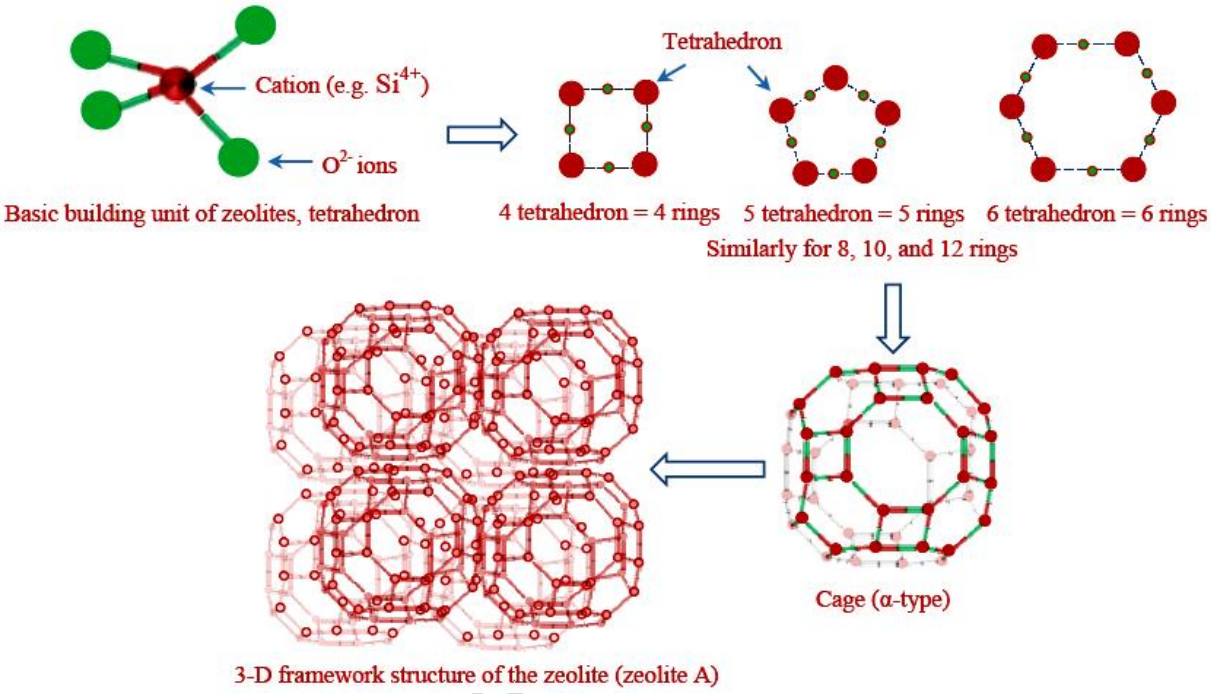

Fig 6: Illustration of zeolite structure formation (Adapted from [151])

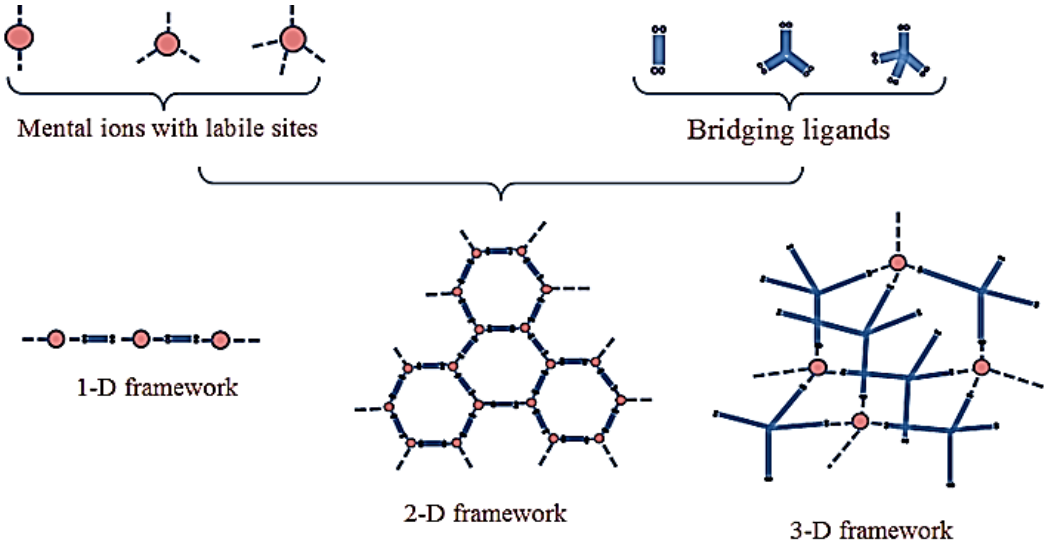

Fig 7: The building block of metal-organic frameworks (Adapted from [182])

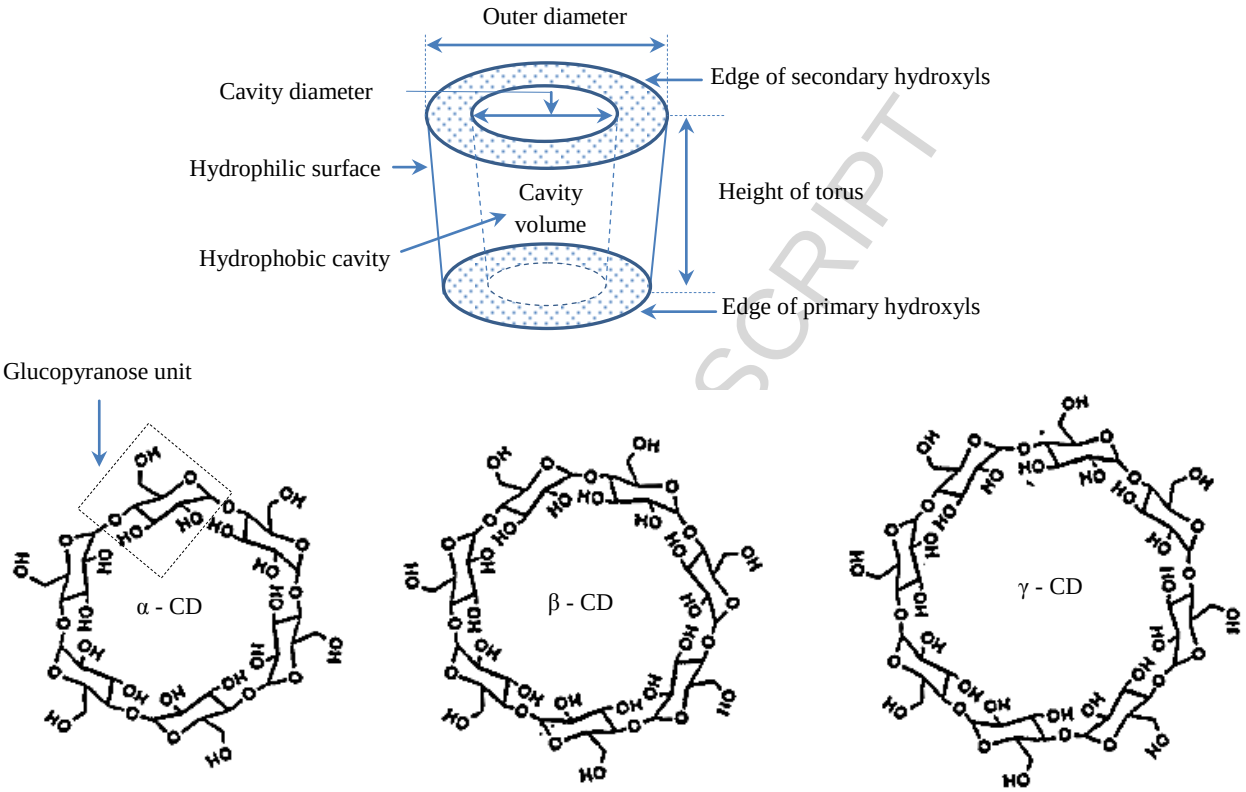

Fig 8: Geometrical dimensions of α-, β-, and γ-cyclodextrin structure (CD = cyclodextrin) [215]

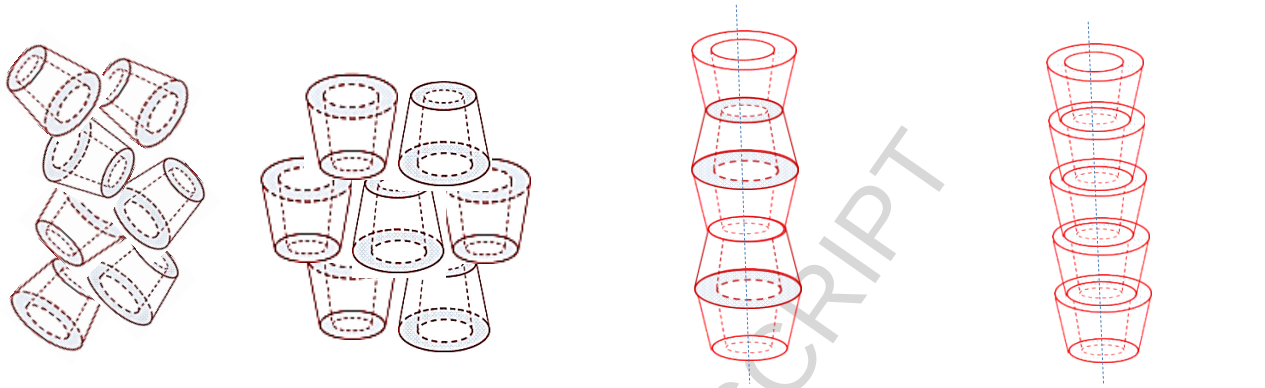

Fig 9: Schemes of possible arrangement of cyclodextrin molecules in crystalline complexes (Adapted from [235])

Graphical abstract

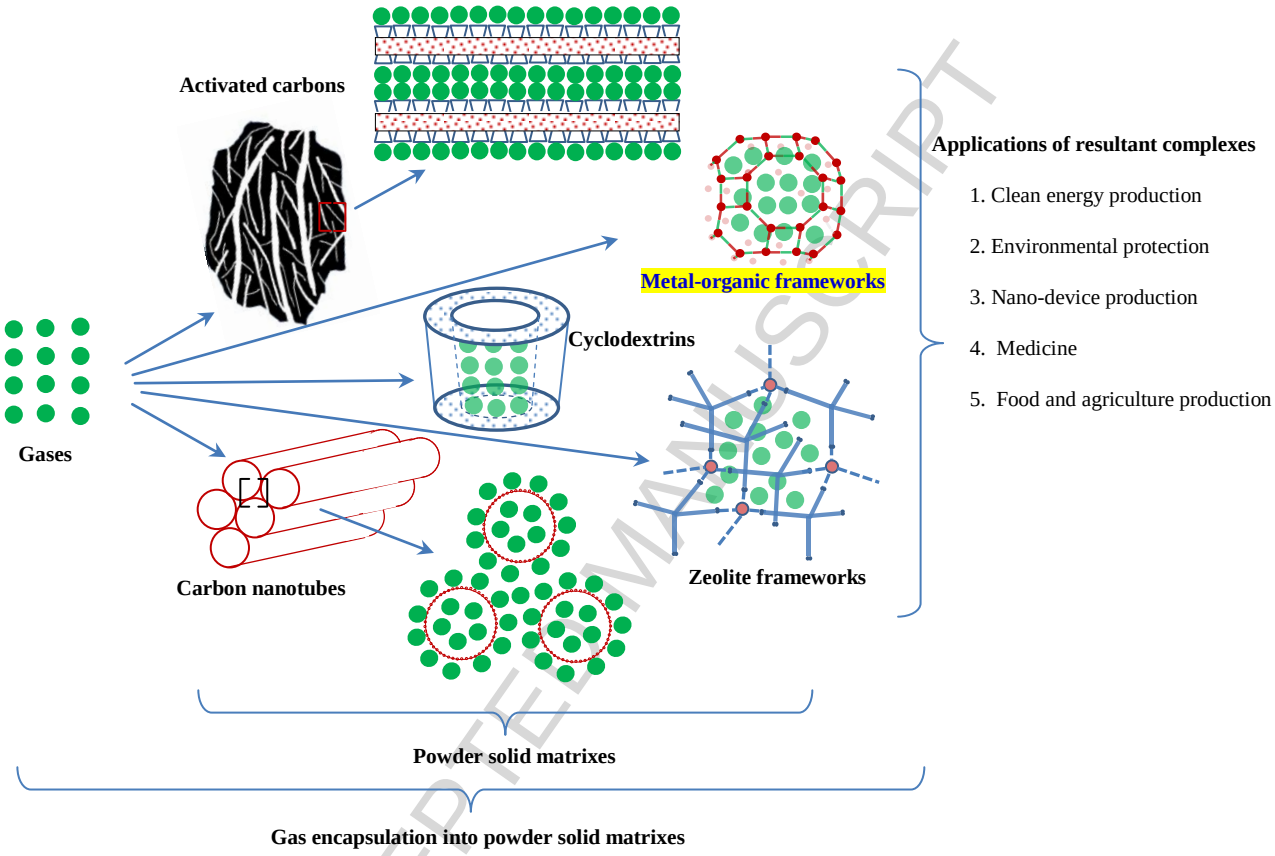

Table 1: Examples of usage of various gases for different functions and products

Gases	Applications
CO_2	Bubble-creating or leavening agent, extension of the shelf-life of dairy products and fruit juices, improvement of food quality, modified atmosphere in food storage, prevention of thrombus formation,
N_2	Modified atmosphere in food storage, space aircraft, the production of ammonia
O_2	Medicine, steel making
CO	Modified atmosphere packaging for meat products, gasotransmitter and therapeutics
H_2	Energy-rich fuel-cell devices
CH_4	Clean energy production
C_2H_4	Fruit ripening and promotion for germination of seeds
N_2O	Canister sprays (non-stick cooking oil, whipped cream), and anaesthesia
SO_2	Anti-browning of fruits and vegetables
1-MCP	Delay ripening of fruits and vegetables
O_3	Water treatment, sanitisation of raw fruits and vegetables
He, Ar & N_2	Analytical equipment (e.g. gas chromatography)
ClO_2	Surface disinfection
NO & H_2S	Gasotransmitter and therapeutics (e.g. platelet aggregation inhabitation and antibacterial activity, modulating cellular functions)

Table 2: Differences between physical and chemical adsorption [34], [35].

Characteristics	**Physisorption**	**Chemisorption**
Nature of binding forces	- Physical forces (dipole-dipole, apolar, electrostatic, hydrophobic associations or Van der Waals) - Polarization - Reversible	- Chemical bonds (covalent, metallic or ionic) - Electron exchange - Irreversible
Heat of adsorption	Low (8-41 kJ $mole^{-1}$ gas, i.e. ~ heat of liquefaction)	High (62-418 kJ $mole^{-1}$ gas)
Effects of temperature on adsorption ability	Decrease with increase in temperature	Increase with increase in temperature
Pressure in which adsorption occurs	Insignificant at low pressure and increase with increase in pressure	Much lower than pressure range of physisorption
Volume of absorbed gases	Depends on boiling point and critical temperature of gases	Independent on boiling point and critical temperature of gases
Saturation uptake	Multilayer adsorption	Monolayer adsorption
Activation energy for desorption	Low	Very high
Kinetics of adsorption	Very variable - often an activated process	Fast - since it is a non-activated process
Selectivity of sorptive gases	Low	High

Table 3: Characteristics and usage of some common adsorption isotherm models

Isotherms (*)	Characteristics	References
Langmuir $q = q_m \frac{b*P}{1-b*P}$	- Two parameter isotherm for noncompetive, nondissociative adsorption - Assumptions: + The surface is homogeneous + Each adsorption site holds only one molecule + There are no interactions between adsorbate molecules	[42]
Freundlich $q = K_F * P^{\frac{1}{n}}$	- Two parameter model - No physical basis for equations (purely empirical and no theoretical basis) - Multilayer adsorption with different distribution of adsorption heat and force over the heterogeneous surface - It does not work well for adsorption on a highly ordered surfaces, only fits adsorption data taken over a small range of pressure and has little predictive value - Ignores interactions between adsorbate and adsorbate - Assumes that adsorbate randomly populates the available adsorption sites - It fails when the concentration of the adsorbate is very high	[42] [43]
Toth $q = \frac{q_m * P}{(b + P^t)^{\frac{1}{t}}}$	- Three parameter model - Empirical equation to describe heterogeneous adsorption systems - The most successful isotherm both at low and high pressure on heterogeneous surfaces - Ignore adsorbate/adsorbate interactions	
Tempkin $q = \left(\frac{R*T}{K_T}\right)\ln(A*C_e)$	- Two parameter model - Accounts interactions between adsorbate and adsorbate - Does not consider how the adsorbate layer is arranged	[41] [44]
BET $q = \frac{q_s * K_{BET} * C_e}{(C_s - C_e)\left[1 + (K_{BET} - 1) * \left(\frac{C_e}{C_s}\right)\right]}$	- Three parameter model, multilayer adsorption - Uniform heat of adsorption (heat of adsorption of the second and subsequent layers is equal to the heat of liquefaction of the solute) - Multiple gas molecules can be adsorbed to each site - Gases in the second and higher layers are assumed to be liquid like - Used for determining pore surface area of solid matrices for gas adsorption	[41] [45]

(*) q is amount adsorbed in equilibrium with the concentration of adsorbate in gas phase (mmol g^{-1} and mg g^{-1} for Tempkin isotherm). q_m is maximum adsorption amount (mmol g^{-1}). P is equilibrium pressure of the adsorbate in gas phase (kPa). b is equilibrium constant of adsorption (kPa^{-1}). K_F is Freundlich constant. 1/n is heterogeneity factor and an indicator for adsorption capacity. t is Toth isotherm exponent related to surface heterogeneity (usually less than or equal to unity). K_T is Temkin constant related to heat of sorption (J $mole^{-1}$). A is Temkin isotherm constant (L g^{-1}). R is gas constant (8.314 J $mole^{-1}$ K^{-1}). T is absolute temperature (K). C_e is amount of adsorbed adsorbate per unit mass of unabsorbed adsorbate concentration in solution at equilibrium (mg L^{-1}). K_{BET} is the BET adsorption isotherm (L mg^{-1}). C_s is adsorbate monolayer saturation concentration (mg L^{-1}). q_s is theoretical isotherm saturation capacity (mg g^{-1}). q_e is equilibrium adsorption capacity (mg g^{-1}).

Table 4: Classification of solid matrices used to entrap gases

Classification basis		Solid matrices				
		Activated carbons (*)	**Carbon nanotubes (*)**	**Zeolites**	**Cyclodextrins**	**Metal-organic frameworks**
Molecular composition	Organic	x	x		x	
	Inorganic	x	x	x		x
Structure	Ordered (crystalline)			x	x	x
	Disordered (non-crystalline)	x	x			

(*) These matrices can be classified as organic or inorganic

Table 5: The studies on gas adsorption using various forms of activated carbons

Gases	Raw materials	Adsorption conditions	Adsorption amount of gas (g $100g^{-1}$)	References
SO_2	ACs (1,036 $m^2 g^{-1}$)	P = 0.101 MPa T = 288.15-306.15 K	0.41-13.40	[82]
	ACF-15 (1,585 $m^2 g^{-1}$)	P = 0.101 MPa T = 393.15 K	11.00	[99]
	NH3-ACF-15 [(a)]		58.00	
CH_4	Coconut shell [(b)]	P = 3.50 MPa T = 298.15 K	10.60-13.40	[100]
	CFC-73	4.00 MPa & 298 K	15.24	[53]
CO_2	AC1 (553 $m^2 g^{-1}$)	P = 1.00 MPa T = 298.15 K	26.00	[101]
	AC2 (809 $m^2 g^{-1}$)		14.70	
	Charcoal (135 $m^2 g^{-1}$)		12.00	
	Coal (100 $m^2 g^{-1}$)		5.50	
CH_4	ACs (1,342 $m^2 g^{-1}$) [(c)]	8.50 MPa & 284.3 K	23.00	[7]
C_2H_6		2.80 MPa & 287.5 K	35.00	
C_3H_8		0.59 MPa & 283.9 K	42.00	
C_4H_{10}		0.15 MPa & 282.2 K	44.00	
CO_2		3.36 MPa & 273.3 K	80.90	
N_2		3.06 MPa & 282.2 K	12.00	
THT [(d)]		$2.03x10^{-5}$ MPa [(*)] & 298.8 K	20.10	
TBM [(e)]		$1.93x10^{-5}$ MPa [(*)] & 298.9 K	8.00	
CO_2	C (1,361 $m^2 g^{-1}$)	P = 0.101 MPa T = 298.15 K	7.00	[90]
	CN800 (1,190 $m^2 g^{-1}$) [(f)]		8.40	
ClO_2	ACs (1,000 $m^2 g^{-1}$) [(g)]	0.101 MPa & 297.15 K	11.00	[25]
Chlorpyrifos	BCA (985 $m^2 g^{-1}$) [(h)]	P = 0.101 MPa T = 283 K	0.18	[92]
	CSA (1,001 $m^2 g^{-1}$)		0.25	
CO_2	Active carbon fiber	P [(k)] = 0.05 MPa T = 323.15 K	4.74	[42]
SO_2			33.64	
NO			4.80	
Cl-VOCs [(l)]	Commercial ACs (856 - 927 $m^2 g^{-1}$)	P = 0.152 MPa T = 308.15 K	20.08	[6]
CO_2	AC (730-2,930 $m^2 g^{-1}$)	P = 0.100 MPa T = 273 K & 300 K	273 K = 35.42 300 K = 20.02	[91]
CH_4	BPL (1,000 $m^2 g^{-1}$)	P = 3.8 MPa T = 300 K	19.80	[102]
	AX-21 (3,000 $m^2 g^{-1}$)		52.80	
CO_2	AC (897 $m^2 g^{-1}$)	2.068 MPa & 300 K	37.40	[55]
CO_2	CACM-32 (1,150-1,330 $m^2 g^{-1}$)	P = 0.101 MPa T = 273 K	16.40	[103]
	PACM-28 (820-1,640 $m^2 g^{-1}$)		16.20	
	C35N400 (1,323 $m^2 g^{-1}$)	0.103 MPa & 309.15 K	7.60	[94]
CF_4	AC (Carbosieve G)	0.10 MPa & 300 K	14.96	[5]
CO_2 CH_4	BPL (1,150 $m^2 g^{-1}$)	2.7 MPa & 273 K	CO_2 = 42.24 CH_4 = 7.70	[60]
	A10 (1,200 $m^2 g^{-1}$)	2.8 MPa & 273 K	CO_2 = 52.80 CH_4 = 9.94	
	Maxsorb (3,250 $m^2 g^{-1}$)	3.3 MPa & 273 K	CO_2 = 143.00 CH_4 = 21.65	
	Norit R1 (1,450 $m^2 g^{-1}$)	2.9 MPa & 273 K	CO_2 = 55.00	
	AC-A (1,207 $m^2 g^{-1}$)	2.3 MPa & 273 K	CO_2 = 52.80 CH_4 = 10.27	

[(a)] NH_3-ACF-15 is treated with ammonia at 1,073 K for 60 min; SO_2 adsorption is carryout out with presence of O_2 and H_2O which induces the conversion of SO_2 to H_2SO_4, resulting in very high SO_2 adsorption capacity. [(b)] Combining chemical activation of coconut shell with H_3PO_4 or $ZnCl_2$ followed by physical activation with CO_2. [(c)] Coal-based, extruded carbon (2 mm diameter pellets), courtesy of Sutcliffe Speakman Carbons Ltd. (UK). [(d) & (e)] Tertbutyl mercaptan (TBM) and tetrahydrothiophene (THT) odorants. [(*)] These are the partial pressures of TBM (6.74 ppmv) and THT (6.95 ppmv) in a mixture with helium at 3.5 MPa pressure. [(f)] C is a wood-based granular carbon manufactured by a phosphoric acid activation process; CN800 is activated carbon modified with ammonia at temperature 1,073 K. [(g)] Pellet diameter (4 mm), density (409 kg m^{-3}), and 2-3% moisture content. [(h)] CSA is coconut shell activated carbon; BCA is bone charcoal activated carbon. [(k)] Partial pressure. [(l)] Chlorinated volatile organic compounds (dichloromethane).

Table 6: Summary of some research on gas encapsulation by using carbon nanotubes (CNs)

Gases	CNs types	Conditions	Gas absorption amount (g $100g^{-1}$)	References
(*) CH_4	(a) SWNT	P = 35.62 MPa T = 273 K	4.00	[133]
	(b) MWNT	P = 3.00 MPa T = 303.15-323.15 K	2.17-3.03	[61]
O_2	SWNT	P = $1.3x10^{-10}$ MPa (c) T = 298.15 K	No oxygen uptake	[134]
(*) SF_6	SWNT	P = 2.07 MPa T = 298 K	119.77	[129]
CO_2	MWNT	P = 0.101 MPa T = 293.15 K C_{in} = 15-50% (d)	4.33-11.40	[131]
(e) H_2	MWNT	P = 0.10 MPa T = 298.15 K	0.25	[135]
	MWNT (*)	P = 20 MPa T = 77.15 K; 150 K & 293 K	293 K = 1.60 150 K = 3.70 77 K = 5.20	[122]
	SWNT	P = 10 MPa T = 298.15 K	4.20	[136]
	Li-doped MWNT	P = 0.101 MPa T = 473.15-673.15 K	2.50	[137]
	SWNT	P = 11 MPa; T = 80 K	8.00	[138]
	SWNT (*)	P = 10.132 MPa T = 77 & 298 K	77 K = 4.50 298 K = 0.90	[139]
	SWNT (*)(*)	P = 7 MPa T = 77 K	33.00	[140]
	K-doped CNT (f)	P = 0.101 MPa T = 313 K	14.00	[141]
	Li-doped CNT	P = 0.101 MPa T = 473-673 K	20.00	
CF_4	SWNT	P = 0.10 MPa T = 300 K	21.12	[5]
CO_2	SWNT (g)	P = 0.107 MPa T = 308.15 K	19.01	[142]
CCl_4	SWNT	P = $1.1x10^{-4}$ MPa T = 224 K	47.68	[57]
Kr		P = $1.2x10^{-4}$ MPa T = 77 K	33.94	
Xe		P = $1.3x10^{-4}$ MPa T = 110 K	55.14	
CH_4	SWNT	P = $1.72x10^{-3}$ MPa T = 78.7 K	7.62	[128]
Kr		P = $2.73x10^{-4}$ MPa T = 77.3 K	34.36	

(a) SWNT is single-walled carbon nanotubes. (*) The values are the results of molecular dynamics simulation. (b) MWNT is multi-walled carbon nanotubes. (c) Measurements are performed in an ultrahigh vacuum chamber. (d) Influent CO_2 concentration. (e) For hydrogen adsorption on carbon nanotubes is well reviewed by Darkrima et al. (2002) [119]. (f) CNT is carbon nanotube. (g) SWNT is purified by a high pressure CO disproportionation (HiPCo) process. (*)(*) The values are the results of molecular dynamics simulation with triangular arrays of open and closed SWCNT of various diameters in a wide range of configurations.

Table 7: Summary of research on gas entrapment into zeolites

Gases	Zeolite types	Adsorption conditions	Adsorbed amount (g $100g^{-1}$)	References
CO_2	3A	5.52 MPa & 623.15 K	15.29	[68]
N_2		12.41 MPa & 623.15 K	5.63	
Ar		12.06 MPa & 623.15 K	8.19	
CH_4	3A	P = 414 MPa T = 623.15 K	6.90	[156]
	HSZ-320	P = 2.60 MPa T = 303.15-323.15 K	1.52-1.98	[61]
	DAY		2.32-2.85	
N_2	KNaA [a]	P = 80 MPa T = 500 K (O_2) & 600 K (N_2)	9.00	[158]
O_2			9.72	
Kr	$(K_{7.08}Co_{2.46})$ - A	P = 3.7 MPa T = 573.15 K	9.72	[159]
	$(K_{6.25}Mn_{2.74})$ - A		7.26	
	$(K_{5.58}Zn_{3.21})$ - A		6.73	
	3A	P = 101.3 MPa T = 723.15-923.15 K	5.00 - 20.00	[157]
	5A		15.00	
N_2	ZSM-5	P = 0.027 MPa (CO_2) & 0.067 MPa (N_2) T = 283.15 K	0.89	[160]
CO_2			5.19	
N_2	NaX BaX	P = 0.81 MPa T = 303.45 K	BaX = 5.27 & NaX = 4.17	[161]
CO			BaX = 11.80 & NaX = 10.60	
[b] H_2	$Cs_{2.5}$-A	P = 13.07 MPa T = 623 K	0.17	[37]
	Na_{12}-A	P = 15.2 MPa T = 623 K	0.04	[162]
CH_4	Na-A [c]	268.5 MPa & 623 K	5.26	[93]
C_2H_4		84.1 MPa & 523 K	4.44	
Ar		268.5 MPa & 623 K	15.91	
Kr		435.7 MPa & 623 K	33.85	
Ar	$Cs_{2.7}Na_8H$-A	P = 60.80 MPa T = 673.15 K	8.90	[163]
Kr	Cs_3Na_8H-A	P = 64.34 MPa T = 673.15 K	20.80	[164]
Ne	4A 5A 13X	P = 2.5-500 MPa [d] T = 298.15 K	4A = 1.97; 5A = 02.71; 13X = 01.46	[77]
Ar			4A = 7.43; 5A = 10.27; 13X = 10.11	
N_2			4A = 6.28; 5A = 07.23; 13X = 08.40	
Kr			4A = 4.36; 5A = 23.30; 13X = 25.48	
CH_4			4A = 2.51; 5A = 04.67; 13X = 04.98	
CH_4	13X	P = 5.0 MPa T = 298 K	9.17	[165]
CO_2			32.44	
N_2			11.81	
N_2	K-CHA [e]	P = 0.133 MPa T = 273 K	0.53	[166]
O_2			1.06	
Ar			2.40	
NO	Co-A	0.101 MPa & 273 K	3.61 - 3.91	[14]
H_2	ZIF-20	P = 0.106 MPa T = 77 K & 87 K	77 K = 0.92 87 K = 0.66	[167]
CO_2		P = 0.106 MPa T = 273 K	13.93	
CH_4			1.22	
CO_2	13X	P = 2.068 MPa T = 300 K	22.90	[55]
	4A		21.10	

[a] Synthesized zeolite A containing 68% K^+ and 32% Na^+. [b] Hydrogen encapsulated in various types of zeolites is summarized in report of Vitillo et al. (2005) [168]. [c] 40% potassium-modified zeolite A. [d] Reported values are the highest adsorbed amount of gas from adsorption isotherm at different pressure ranges. [e] Chabazite with Si/Al of 2.4 ratios was synthesized and exchanged with cations K^+.

Table 8: Gas adsorption by using metal-organic framework solid matrices

Gases	MOF types	Adsorption conditions	Adsorption amount (g $100g^{-1}$)	References
H_2	MIL-53 $BNH_{1.3}$@MIL-53 [(a)] $BNH_{1.7}$@MIL-53	P = 0.109 MPa T = 77 K	MIL-53 = 1.52 $BNH_{1.3}$@MIL-53 = 1.94 $BNH_{1.7}$@MIL-53 = 2.15	[190]
CO_2		P = 0.104 MPa T = 273 K	MIL-53 = 15.80 $BNH_{1.3}$@MIL-53 = 18.90 $BNH_{1.7}$@MIL-53 = 20.20	
H_2	$Zn(bdc)(ted)_{0.5}$ [(b)] $Ni(bodc)(ted)_{0.5}$ $Zn_2(bpdc)_2(bpee)$	P = 4.10 MPa T = 300 K	$Zn(bdc)(ted)_{0.5}$ = 0.33 $Ni(bodc)(ted)_{0.5}$ = 0.26 $Zn_2(bpdc)_2(bpee)$ = 0.092	[201]
	CPO-27-M [(c)] (M = Ni, Co & Mg)	P = 0.10 MPa T = 77 K	CPO-27-Mg = 2.56 CPO-27-Co or Ni = 2.25	[202]
NO	Co-MOF [(d)] Ni-MOF	P = 0.10 MPa T = 298.15 K	Co-MOF = 19.60 Ni-MOF = 21.10	[13]
H_2	HKUST-1 [(e)]	P = 0.1 & 1 MPa T = 77 K	0.1 MPa = 2.27 1.0 MPa = 3.63	[173]
NO		P = 0.10 MPa and T = 196 & 298 K	196 K = 27.10 & 298 K = 9.00	
CO_2	Mg-MOF-74 [(f)]	P = 0.102 MPa & T = 298 K	9.77	[195]
	$Zn_2Atz_2(ox)$ [(g)]	P = 0.12 MPa & T = 273 K	18.90	[203]
	CPO-27-Ni [(h)]	P = 0.101 MPa T = 303, 313 & 353 K	353 K = 12.40 313 K = 25.00 303 K = 29.90	[194]
	MIL-101 [(k)]	P1 = 0.015 MPa P2 = 0.100 MPa T1 = 298.15 K T2 = 323.15 K	P1 : T1 = 1.45 & T2 = 0.88 P2 : T1 = 7.04 & T2 = 4.40	[189]
	PEI-MIL-101-50		P1 : T1 = 10.56 & T2 = 8.19 P2 : T1 = 17.60 & T2 = 13.51	
	PEI-MIL-101-75		P1 : T1 = 16.15 & T2 = 13.95 P2 : T1 = 20.42 & T2 = 17.69	
	PEI-MIL-101-100		P1 : T1 = 18.48 & T2 = 14.96 P2 : T1 = 22.01 & T2 = 18.22	
	PEI-MIL-101-125		P1 : T1 = 16.94 & T2 = 17.38 P2 : T1 = 19.14 & T2 = 19.85	
CH_4	IRMOF-6	P = 3.648 MPa & T = 298 K	17.10	[204]
CH_4	CD-MOF-2 [(l)]	P = 0.107 MPa & T = 298K	0.50	[205]
CO_2		P = 0.107 MPa & T = 273-298 K	11.80 - 15.10	
H_2 & N_2	Mg-MOF [(m)]	P = 0.101 MPa & T = 77 K	H_2 = 5.61 & N_2 = 0.53	[206]
H_2	MOF-177 [(n)]	P = 0.101 MPa & T = 77 K	H_2 = 1.52	[207]
O_2 & N_2		P = 0.101 MPa & T = 298 K	N_2 = 0.30 & O_2 = 0.60	
H_2	MOF-177	P = 7.0 MPa & T = 77 K	7.50	[208]
	IRMOF-1	P = 5.0 MPa & T = 77 K	5.30	
	IRMOF-6	P = 5.0 MPa & T = 77 K	4.90	
	IRMOF-11	P = 3.4 MPa & T = 77 K	3.50	
	IRMOF-20	P = 8.0 MPa & T = 77 K	6.70	
	HKUST-1	P = 8.0 MPa & T = 77 K	3.30	
	MOF-74	P = 2.6 MPa & T = 77 K	2.30	
CO_2 & CH_4	Zn-MOF	P = 0.10 MPa & T = 273 & 300 K	CO_2 =10.40 (273 K) & 8.20 (300 K) CH_4 = 1.90 (273 K) & 1.40 (300 K)	[209]
H_2		P = 0.1 MPa & T = 77-87 K	0.86-0.96	
H_2S	MIL-47(V) MIL-100(Cr) MIL-101(Cr)	P = 1.60 MPa T = 303.10 K	MIL-47(V) = 47.70 MIL-100(Cr) = 57.90 MIL-101(Cr) = 129.50	[210]
	Ni-CPO-27	P = 0.101 MPa & T = 298.15 K	40.90	[211]
NH_3	HKUST-1	P = 0.101 MPa & T = 298.15 K	11.50-17.20	[212]

[(a)] $BNH_{1.3}$@MIL-53 & $BNH_{1.7}$@MIL-53 are MIL-53 incorporated 1.3 wt% & 1.7 wt% ammonia borane respectively. [(b)] bdc is 1,4-benzenedicarboxylate, ted is triethylenediamine, bodc is bicyclo[2.2.2]octane-1,4-dicarboxylate, bpdc is 4,4′-biphenyldicarboxylate, bpee is 1,2-bipyridylethene. [(c)] $M_2(dhtp)(H_2O)_2.8H_2O$ with dhtp is 2,5-dihydroxyterephthalic acid. [(d)] $[M_2(C_8H_2O_6)(H_2O)_2].8H_2O$. [(e)] Copper benzene tricarboxylate MOFs. [(f)] Mg_2(DOT) with DOT is 2,5-dioxidoterephthalate. [(g)] Atz is 3-amino-1, 2, 4-triazole & ox is oxalate. [(h)] $Ni_2(dhtp)(H_2O)_2.8H_2O$ & dhtp is 2,5-dihydroxyterephthalic acid. [(k)] MIL-101 loaded with 50, 75, 100 & 125% of polyethyleneimine (PEI). [(l)] CD-MOF-2 consisting of the renewable cyclic oligosaccharide γ-cyclodextrin and RbOH. [(m)] $[Mg_2(HL)_2(H_2O)_4]H_2O]n$ and $[H_3L]$ is 3,5-pyrazoledicarboxylic acid. [(n)] By adding a H_2 dissociating catalyst and using a bridge building technique to build carbon bridges for hydrogen spillover.

Table 9: The basic properties of α-, β-, and γ-cyclodextrin

Properties	**α-cyclodextrin**	**β-cyclodextrin**	**γ-cyclodextrin**	**References**
Empirical formula (anhydrous)	$C_{36}H_{60}O_{30}$	$C_{42}H_{70}O_{35}$	$C_{48}H_{80}O_{40}$	[216]
Number of glucopyranose units	6	7	8	[217]
Molecular weight (g $mole^{-1}$)	973	1135	1297	
Solubility in water at 298.15 K (g $100mL^{-1}$)	14.5	1.85	23.2	
Outer diameter (nm)	1.64	1.54	1.75	
Cavity diameter (nm)	0.47-0.53	0.60-0.65	0.75-0.83	
Height of torus (nm)	0.79	0.79	0.79	
Cavity volume of 1 molecule (nm^3)	0.174	0.262	0.427	
Cavity volume of 1 molecule (mL)	104	157	256	[218]
Cavity volume of 1 gram (mL)	0.10	0.14	0.20	

Table 10: Summary of some research on gas encapsulation by using cyclodextrins

Gases	Cyclodextrin	Encapsulation conditions	Encapsulation amount (g $100g^{-1}$)	References
C_2H_4	α- cyclodextrin	P = 0.2-1.5 MPa T = 298.15 K	2.74-2.88	[79]
CO_2		P = 1-3 MPa T = 298.15 K	4.20-4.66	[225]
CO_2	β-CD nanosponges [(a)]	P = 0.10 MPa T = 293.15 K & 393.15 K	293.15 K = 0.40 393.15 K = 0.60	[226]
1-MCP		Directly bubbling in water suspension of nanosponges (0.101 MPa, 298.15K)	8.10-9.10	
Cl_2	α- cyclodextrin	P = 0.7-12 MPa T = 293.15 K	2.14	[227]
Kr			2.84	
Xe			10.27	
O_2			1.04	
CO_2			5.87	
C_2H_4			1.81	
CH_4			1.62	
C_3H_8			4.43	
C_4H_{10}			6.69	
1-MCP	α- cyclodextrin	P = 0.101 MPa T = 288.15 K	5.02	[225]

[(a)] Cross-linking of cyclodextrin with carbonildiimidazole

Table 11: Potential application of gas encapsulated in various solid matrices

Complexes	Potential applications					
	Emission control	**Clean energy production**	**Pharmacy**	**Removal of harmful gases**	**Nano-devices production**	**Food & agricultural production**
Activated carbons	x	x		x		
Carbon nanotubes	x	x		x	x	
Cyclodextrins						x
Zeolites	x	x	x	x		
Metal-organic frameworks	x	x	x	x		

Highlights

- We present current status of gas encapsulation in various powder solid matrices.
- We describe molecular structure of solid matrices and gas adsorption mechanism.
- The gas storage capacity of various solid matrices is compared.
- Adsorption isotherm and release property of gases from matrices are described.
- We discuss potential applications of resultant complexes in various fields.